RESEARCH

UDOT

Keeping Utah Moving

Utah Department of Transportation - Research Division
4501 South 2700 West - P.O. Box 148410 - SLC,UT 84114-8410

Report No. UT-21.23

SALT LAKE CITY AIRPORT PARKING GARAGE VISUAL INSPECTION REPORT

Prepared For:

Utah Department of Transportation
Research & Innovation Division

Final Report
August 2021

DISCLAIMER

The authors alone are responsible for the preparation and accuracy of the information, data, analysis, discussions, recommendations, and conclusions presented herein. The contents do not necessarily reflect the views, opinions, endorsements, or policies of the Utah Department of Transportation or the U.S. Department of Transportation. The Utah Department of Transportation makes no representation or warranty of any kind, and assumes no liability, therefore.

ACKNOWLEDGMENTS

The authors acknowledge the Utah Department of Transportation (UDOT) and the American Concrete Institution (ACI) Foundation for funding this research. The authors also thank the ACI International Correspondents (Kyle Stanish of Committee 365 Service Life Prediction, and Rachel Detwiler, Fouad Yazbeck, and R. Doug Hooton of Committee 234 Silica Fume in Concrete), ACI Intermountain Chapter Industry Advisors for this project (Tammy Meldrum, Kevin Robins, Jeff Tanabe, Mike Buehner, Jerry Hall, and Todd Laker), and UDOT Technical Advisory Committee Members (Bill Lawrence, Bryan Lee, James Corney, and Vincent Liu) who helped support and guide the research. We also thank W. Spencer Guthrie, Brian Mazzeo, and their research undergraduate and graduate students at Brigham Young University who assisted in the gathering of the test samples for this project. The authors thank Tanner Durfee for assisting in crack mapping and doing additional literature review research on supplementary cementitious materials and parking garages as part of his Utah Valley University senior capstone class.

TECHNICAL REPORT ABSTRACT

1. Report No. UT-21.23	2. Government Accession No. N/A	3. Recipient's Catalog No. N/A
4. Title and Subtitle Salt Lake City Airport Parking Garage Visual Inspection Report		5. Report Date August 2021 6. Performing Organization Code
7. Author(s) Amanda Bordelon, Madison Clyde, and Thomas Gwynn		8. Performing Organization Report No.
9. Performing Organization Name and Address Utah Valley University Department Engineering 800 W University Parkway Orem, UT 84058		10. Work Unit No. 5H08603H 11. Contract or Grant No. 21-8223
12. Sponsoring Agency Name and Address Utah Department of Transportation 4501 South 2700 West P.O. Box 148410 Salt Lake City, UT 84114-8410		13. Type of Report & Period Covered Final September 2020 - October 2020 14. Sponsoring Agency Code PIC No. UT20.103

15. Supplementary Notes
Prepared in cooperation with the Utah Department of Transportation and the U.S. Department of Transportation, Federal Highway Administration

16. Abstract

An overall project was initiated to determine whether the use of micro-silica slurry as a supplementary cementitious material was significantly beneficial at creating a low permeability corrosion-resistant concrete, particularly from the inspection of the old parking garage at the Salt Lake City Airport. This report outlines the initial visual and some non-destructive inspection methods used to assess the parking garage. This parking garage is unique since it was one of the oldest structures in the United States built with silica fume as a pozzolan in the concrete.

A history of the structure is summarized in the report. Cracking found in the structure was mostly epoxy-filled, and anecdotally noted to have been filled during the original construction. The only maintenance on record in the structure since construction was stated to be power-washing, which is very low maintenance for this type of parking garage structure. The visual inspection of the structure indicates that the parking garage's crack density was lower than most UDOT bridge structures, which can be attributed to either the use of silica or the enhanced reinforcement (epoxy rebars and post-tensioned steel). Schmidt hammer tests verified the concrete was extremely strong, > 20ksi even for sections of concrete with no silica added. Further tests will be conducted to determine the concrete's chloride permeability and content. This data will help determine if the silica fume has maintained its low permeability and high strength properties over time.

17. Key Words Concrete; Silica Fume; Parking Garage; Visual Inspection; Airport; Schmidt Hammer; Cover Meter Depth; Crack Density		18. Distribution Statement Not restricted. Available through: UDOT Research Division 4501 South 2700 West P.O. Box 148410 Salt Lake City, UT 84114-8410 www.udot.utah.gov/go/research	23. Registrant's Seal N/A
19. Security Classification (of this report) Unclassified	20. Security Classification (of this page) Unclassified	21. No. of Pages 85	22. Price N/A

TABLE OF CONTENTS

LIST OF TABLES

LIST OF FIGURES

LIST OF ACRONYMS

BYU	Brigham Young University
EB	Eastbound
FHWA	Federal Highway Administration
GPR	Ground Penetrating Radar
NB	Northbound
NDE	Non-Destructive Evaluation
OPC	Ordinary Portland Concrete
PT	Post-Tensioned
RCPT	Rapid Chloride Permeability Test
SB	Southbound
SFC	Silica Fume Concrete
SLC	Salt Lake City
SOG	Slab-On-Grade
UDOT	Utah Department of Transportation
U of T	University of Toronto
UVU	Utah Valley University
VEI	Vertical Electrical Impedance
WB	Westbound

EXECUTIVE SUMMARY

This report summarizes the history and on-site inspection performed at 29 years of age on the old Salt Lake City (SLC) airport parking garage. This structure was unique at its time to have 9% micro-silica slurry added to the concrete mix. In combination with unbonded post-tensioned cables and epoxy-coated rebar, the structure was expected to have a long service life and low corrosion. In discovering the history of the structure, it was noted that all concrete batch information was lost to a fire, and thus much of the historical summary is based on anecdotal recollections. This report also has a brief literature review comparing the parking garage to similar bridges or parking garages found in the United States with similar mixtures or reinforcement.

The report focuses on the detailed descriptions of the visual inspection performed on the SLC airport parking garage structure in September and October 2020 before it was demolished. The initial visual inspection included crack mapping of the entrance bridge, three suspended slab levels, the ground slab-on-grade, and the two helix ramps. Cracks were measured or estimated from both the top surface and those that were viewed from underneath the slab, where applicable. Efflorescence or leaching was observed and also indicated on the crack maps. Crack densities were calculated and reported for the various structure sections.

In addition to crack mapping, five locations (one from each floor and ramp) were selected for more thorough non-destructive evaluation (NDE) measurements. These NDE methods included: Schmidt hammer for strength estimation, cover meter for reinforcement location and depth, ground penetrating radar (GPR) for mapping reinforcement, chain drag for delamination locations, and vertical electrical impedance (VEI) scanning for corrosion potential. At these five locations, some semi-destructive methods were performed to collect samples of the concrete to

take back to the lab for further measurements. These semi-destructive methods included roughly 3-6 cores and 6-12 drilled profile sites from each location. The powder from the drilled profiles was collected at 1-inch depth intervals, up to 7 inches or the bottom of the slab. Half of the drilled profiles were over a crack or saw-cut joint, with the other half were obtained four inches from a crack or joint. The cores and powder samples will be analyzed in future work. GPR and VEI data will also be summarized in a separate report.

1.0 INTRODUCTION

1.1 Problem Statement

The old SLC International Airport's parking garage (shown in Figure 1-1 and Figure 1-2) was built in 1989-1991 and incorporated unique technologies at its time, primarily the use of a micro-silica slurry in the concrete to enhance the resistance of chloride migration that can corrode the reinforcement. The parking garage was demolished in the fall of 2020 to make room for a new airport terminal expansion (location of the new airport shown in Figure 1-3). Before the parking garage was demolished, various non-destructive tests, core samples, and chemical analysis samples were obtained with the interest in characterizing the performance of the silica fume especially as to whether it reduced the chloride ingress in the structure.

Figure 1-1 Aerial photograph of the SLC airport and parking garage obtained from Bing.com, image from 2020 before demolition began.

Figure 1-2 3D rendering looking north onto the parking garage, obtained from Google Maps, image from 2020 before demolition began.

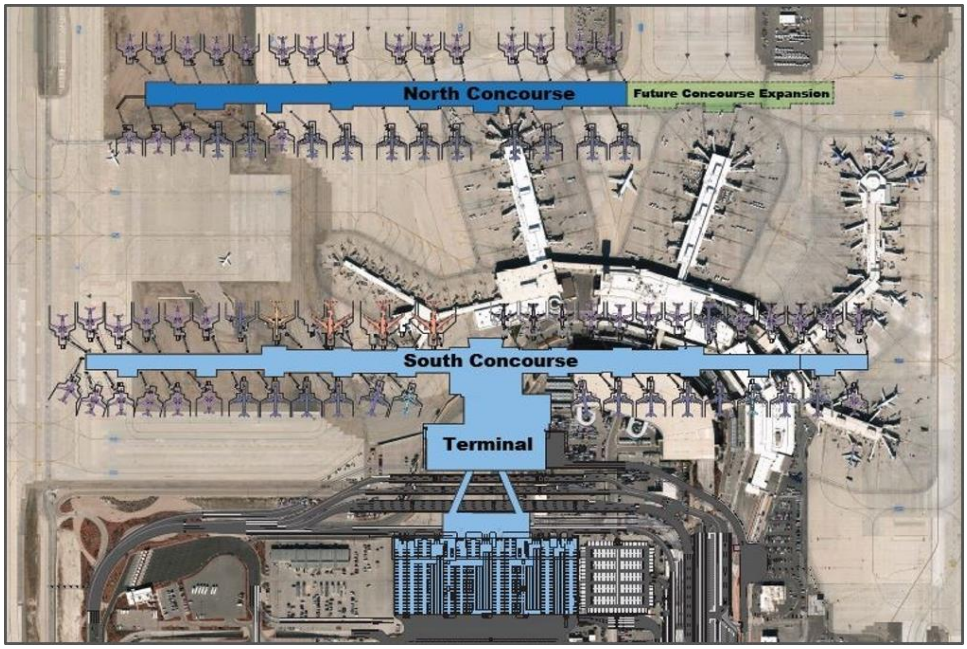

Figure 1-3 Location of new SLC airport terminal, concourses, and parking garage (all in blue) superimposed over the location of the old SLC airport and parking garage (in white or tan). The new airport's south concourse will be through the location of the parking garage, hence why it will be demolished.

1.2 History of the Parking Garage

The parking garage was designed by MHTN Architects and Reaveley Engineers in 1989 and opened for use in 1991. The parking garage was unique because it was among the first structures in the United States built with a micro-silica slurry, used as a supplementary cementitious or pozzolanic material. The parking garage was designed to have a 75-year design life due to the low permeability and high strength characteristics that the silica fume added to the concrete, in addition to the epoxy-coated rebar and polymer coated post-tensioned steel reinforcement system.

1.2.1 Project Schedule

In early 2019, the American Concrete International Intermountain Chapter heard news that the SLC Airport Parking Garage would be demolished to make way for a new airport terminal. A task group was arranged to delegate and find financial support to investigate the parking garage because of its unique aspects. The parking garage was in great condition, but at only half of its service life span. One of the first task items was capturing the history of the structure. A meeting was held on June 11, 2019 with representatives from the various parties involved in the original design, construction, and testing of the airport. The information gathered from that session is presented herein. Structural and architectural drawings were obtained from Reaveley Engineers. Unfortunately, the original mix design and batch tickets were lost in a fire, so the details on the mix design come from the anecdotal recounts of what occurred from 1988-1991. The SLC Airport, and later the demolition contractor HDJV, became involved in the process and planning of what could be done to gather information on the structure before it was demolished.

The same parking garage was tested at 12 years of service life as part of a study funded through the Silica Fume Association to quantify the benefit of silica on chloride penetration, carbonation depth, and diffusion in bridge decks and parking garages. Additional information from that study (Bentz and Hooton, 2008; Hooton et al., 2010) was gathered to be combined with the planned similar test results obtained in this research for the structure at 29 years of service life.

In this study, the actual on-site investigation was limited to only the narrow time frame from after the SLC Airport had vacated the parking garage, to when the demolition contractor began tearing down the structures. In this narrow window, the team was able to visit the structure four times in 2020 to do all the measurements and obtain samples: August 14 (parking garage still in use at time), September 17, September 30 (after demolition of entrance bridge), and October 8 (after demolition of structure D). During an additional site visit on November 4 (after demolition of structure A), a few samples of steel reinforcement bars and post-tension tendons were gathered to test in a future project.

1.2.2 Structure Details

The parking garage structure shown in Figure 1-4 was built using four separate suspended slab-and-column structures, A-D, two one-lane, center-supported, cantilevered helix ramps, two entrance/exit ramps, and an entrance bridge. The elevated structures, helix ramps, and bridge were all used by short-term daily vehicle parking. The structure's slab-on-grade (SOG) ground floor was used for rental cars and had its own entrance and exit instead of connecting to the helix ramps. All levels were covered; the top floor was covered with a metal roof. The sides of the parking garage elevated slabs, entrance ramp, and helix ramps had a sidewalk or curb and a four-foot-tall, pre-cast, reinforced concrete wall panel tied into the structure.

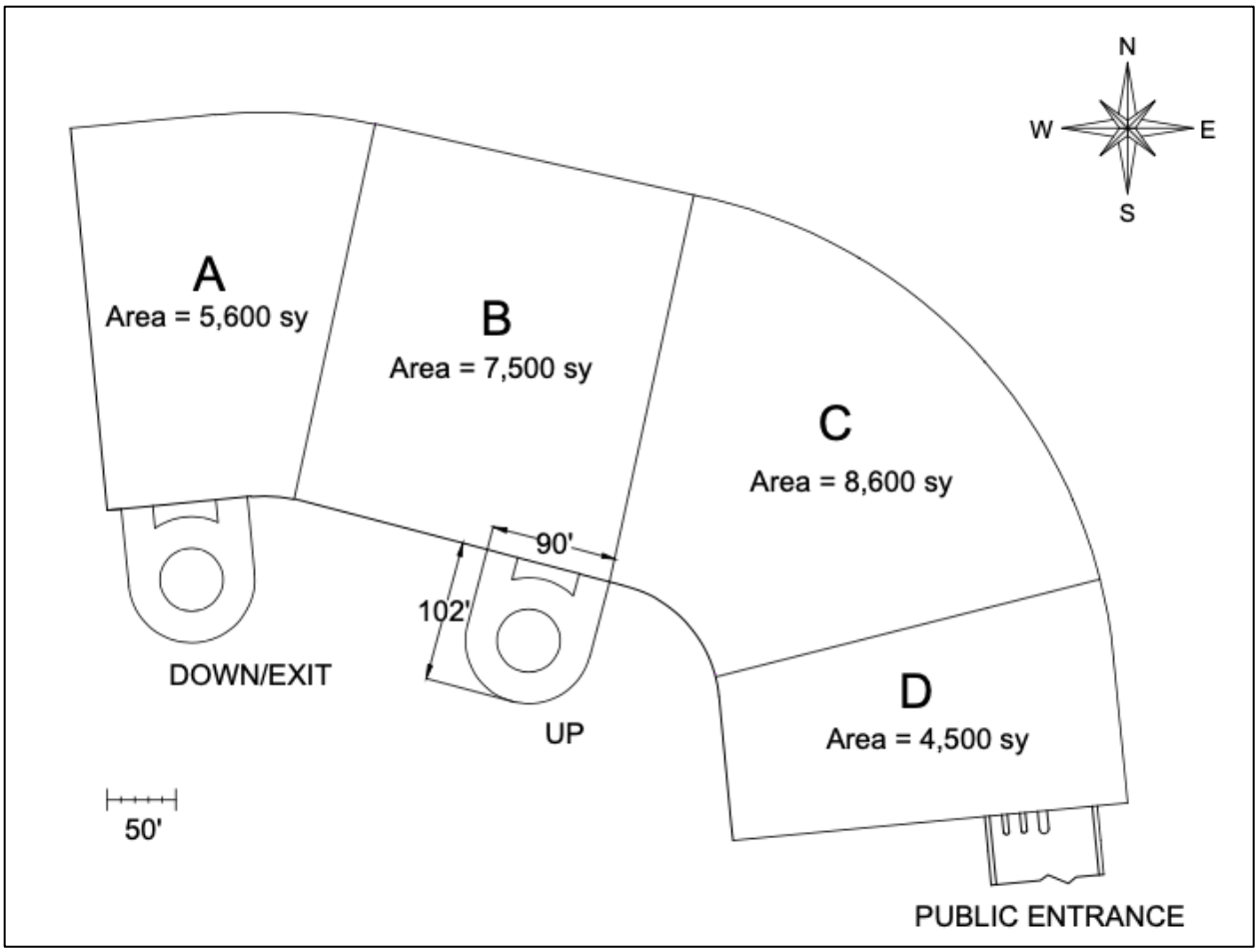

Figure 1-4 Parking garage layout of the first floor showing each structure A-D location and size, as well as the location and size of the entrance ramp and helix ramps.

Each level had 194 columns, each 36-inch diameter with twelve #11 vertical reinforcement bars and spirals 5/8-inch diameter and 2- to 3-inch pitch. A diagram of the parking garage simplified to show the column locations can be seen in Figure 1-5. The columns are spaced 54 feet apart to accommodate for each of the five driving lanes (A-F) and roughly 30 feet apart longitudinally (1-38).

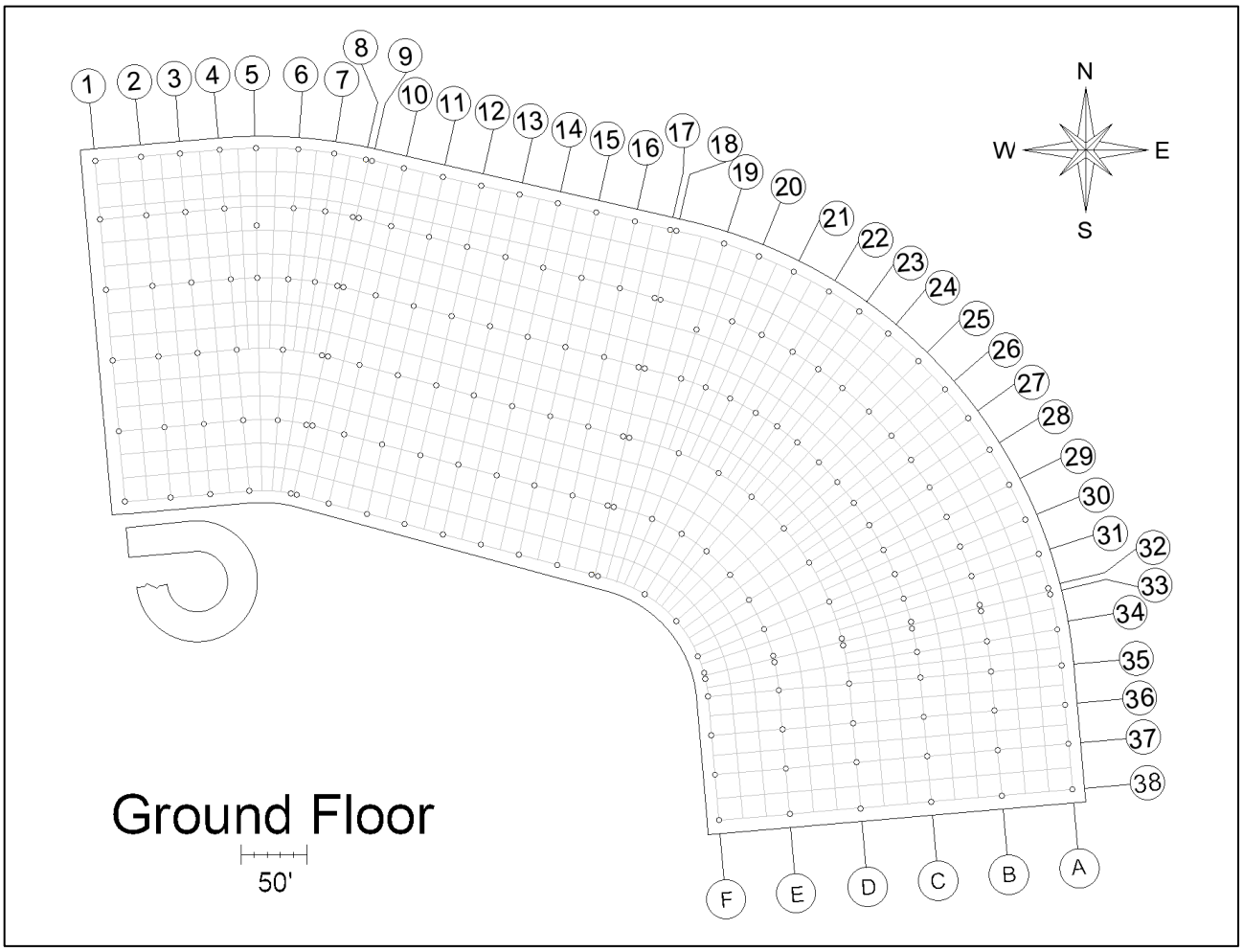

Figure 1-5 Parking garage layout of the ground floor SOG showing the column location identification A-F and 1-38. Saw-cut joints (only on ground floor) are shown as the gray lines between columns.

Underneath each column was a 38- to 69-inch-thick concrete pile cap and anywhere from 6 to 19 piles. The piles were each 12-inch diameter, with 3/8-inch wall thickness and went down 65 feet. In the pile arrangement under each cap, the perimeter piles were battered with a slope of 3’/10’ and all interior piles were vertical. Pile caps were connected horizontally with reinforced concrete tie beams typically 16 inches wide and 24 inches deep.

The helix structures had a center interior support column of 7.5 feet diameter, a concentric interior wall at 38 feet diameter, radial spoke beams and concentric beams that extend from the

interior support column out to a diameter of 92 feet. The outer portion 23 feet is a driving loop only supported by the beams, with an inner curb and railing and outer pre-cast wall panel similar to the rest of the parking garage. There was a 4-foot gap between the concentric inner wall and the edge of the driving loop. The six radial beams containing reinforcement and post-tensioning were 36 inches tall at the exterior end and 60 inches tall at the interior column; these are 30 inches wide. There are three concentric beams that are 36 inches tall and 12 to 24 inches wide. The three concentric beams are evenly split across the outer 23-foot-wide driving loop portion of the structure. The concentric interior wall is 12 inches thick and reinforced with #4 bars at 12 inches on center each way. The helix ramp structures similarly had 176 piles underneath the center column and concentric interior wall.

An exit ramp was originally built on the far northwest corner of leaving from the first floor. This exit ramp was removed in February 2016 and is not shown in Figure 1-4. Entrance to the short-term parking in the garage remained for the majority of the visual inspection period, this entrance ramp consisted of an uncovered SOG and uncovered entrance bridge deck on the south side of the parking garage, shown as the public entrance in Figure 1-4. Vehicles exiting since 2016 were rerouted directly from the down/exit helix, as indicated in Figure 1-5, to the nearby terminal drive.

The largest unsupported diagonal span was 60 ft. The reinforced beam and column suspended slabs varied in thickness from 7 inches to 15 inches throughout the structure. The reinforced and beam-supported helix ramp and entrance bridge slab were both 8 inches thick. The unreinforced ground floor SOG was designed at 7 inches thick. In general, the beams in the suspended slab structure were 30 to 36 inches wide and all were 36 inches deep. The beams

contained post-tensioning at 226 to 935 kips force and had epoxy-coated rebar of five to eight #8 to #10 bars with #4 stirrups.

1.2.3 Reinforcement in Slabs

The concrete for the suspended slabs, entrance bridge, and helixes were reinforced in two directions using both epoxy-coated rebar and unbonded post-tensioned cables. All reinforcement including deformed bars, tendon cables, support bars, chairs, and tie wires were coated in either epoxy or plastic.

The epoxy-coated deformed bar consisted of a Grade 60 mild steel of yield strength 60 ksi. The following are details of the rebar in the various structures:

- suspended slabs were No. 4, varying from 3.5 to 14 inches on center,
- helix ramps were No. 4 at 16 inches on center, and
- entrance bridge was No. 7 at 5 inches on center near the top or 6 inches on center near the bottom of the slab.

An example of the epoxy rebar layout can be seen in Figure 1-6 for structure D, in Figure 1-7 for the bridge, and a profile view and lapping of rebar in Figure 1-8. The structural drawings required a 2-inch minimum cover depth for all reinforcing bars.

Post-tension (PT) cables were comprised of seven wire strands (each strand was a grade 270 low relaxation steel), twisted (each tendon was 0.5 to 0.6 inches diameter), and housed in a greased (unbonded) plastic sheathing. The PT cables were placed every 3.5 to 7.5 feet, based on the thickness of the slab and proximity to nearby reinforcement on beams. End anchors for the tendons were embedded 2 inches on beam ends and 1.5 inches on slab edges then covered by concrete to protect from the elements. The PT system was laid over support chairs prior to casting

in a draped pattern such as that shown in Figure 1-9, where the cables were higher over the underlying beam supports and lowest at mid-span between supports. According to the structural drawings, the cover depth on PT cables was required to be anywhere from 3.75 to 5.75 inches from the top surface, or 1.25 to 2 inches from the bottom surface. For example, see Figure 1-10 for the PT layout on the bridge, or Figure 1-11 for the PT layout on a slab in structure D.

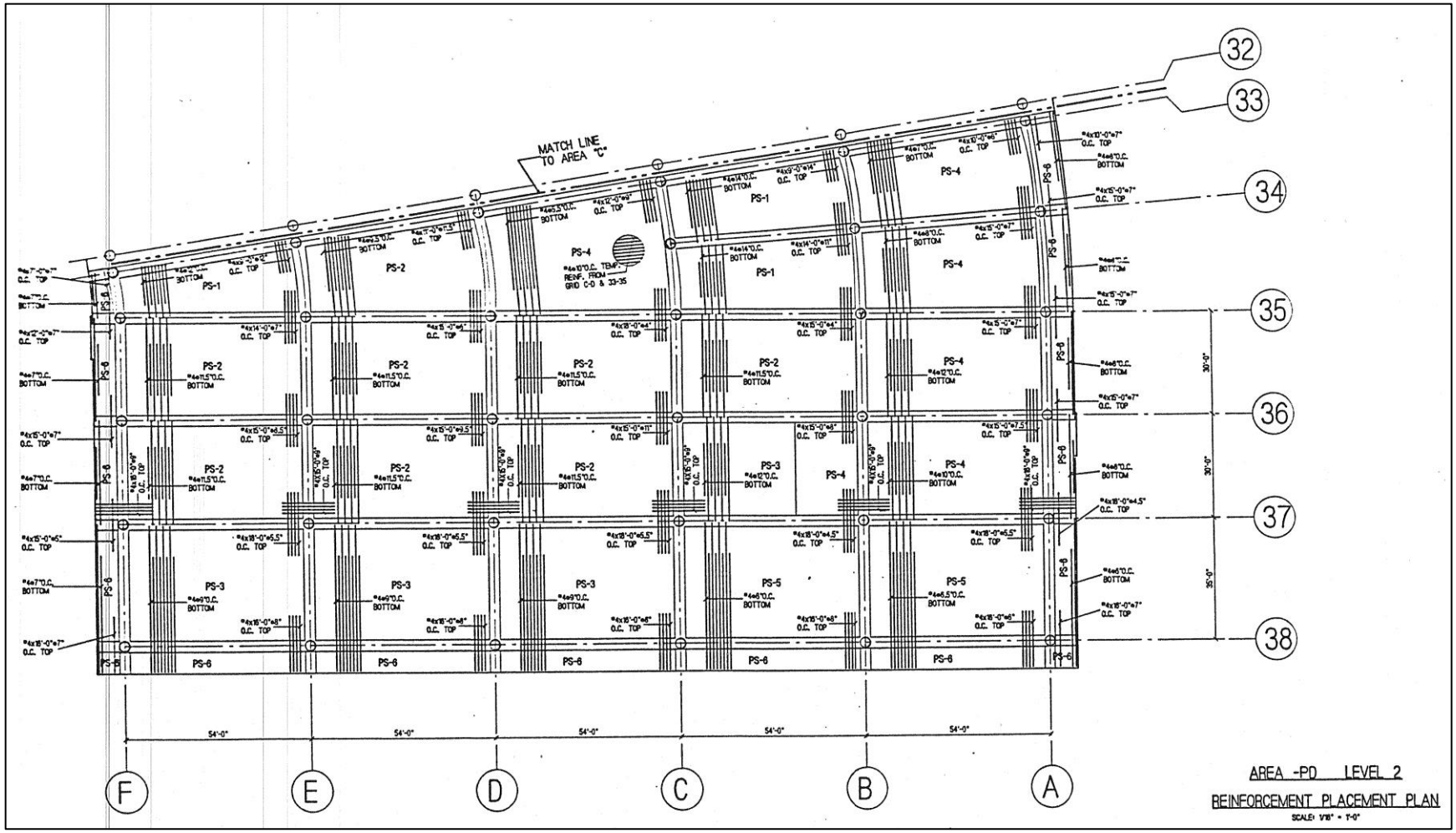

Figure 1-6 Example of the as-built structural drawings from 1988 showing the first floor ("level 2" on drawing) epoxy-coated rebar reinforcement system in structure D (the southeast corner).

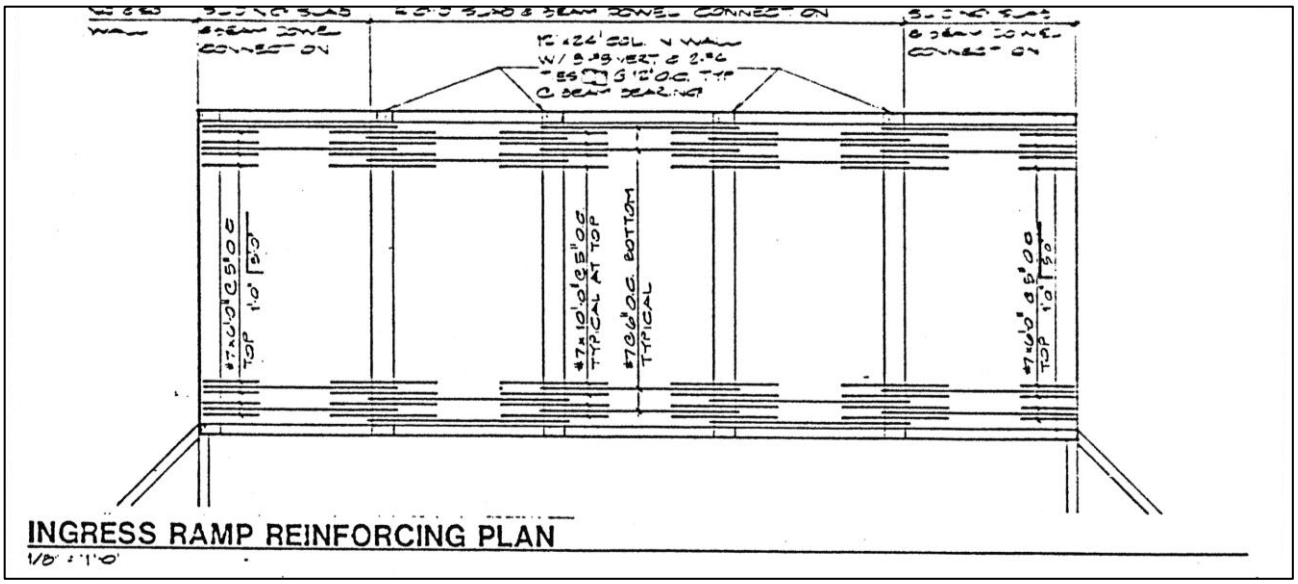

Figure 1-7 Example of the as-built 1988 structural drawings showing the epoxy reinforcement in the entrance ("ingress") bridge from the ingress ramp to the first floor of the garage.

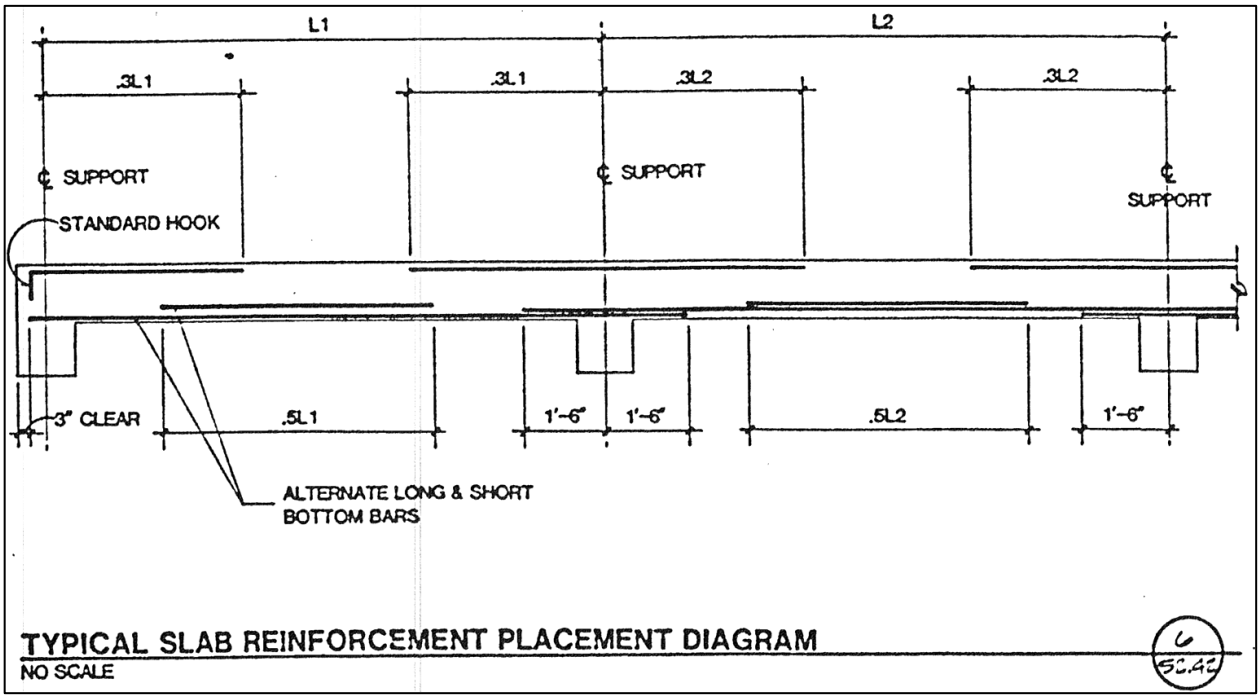

Figure 1-8 Schematic of the epoxy-coated rebar running through the slab across beam supports and at the end of the slab, from the as-built 1988 structural drawings.

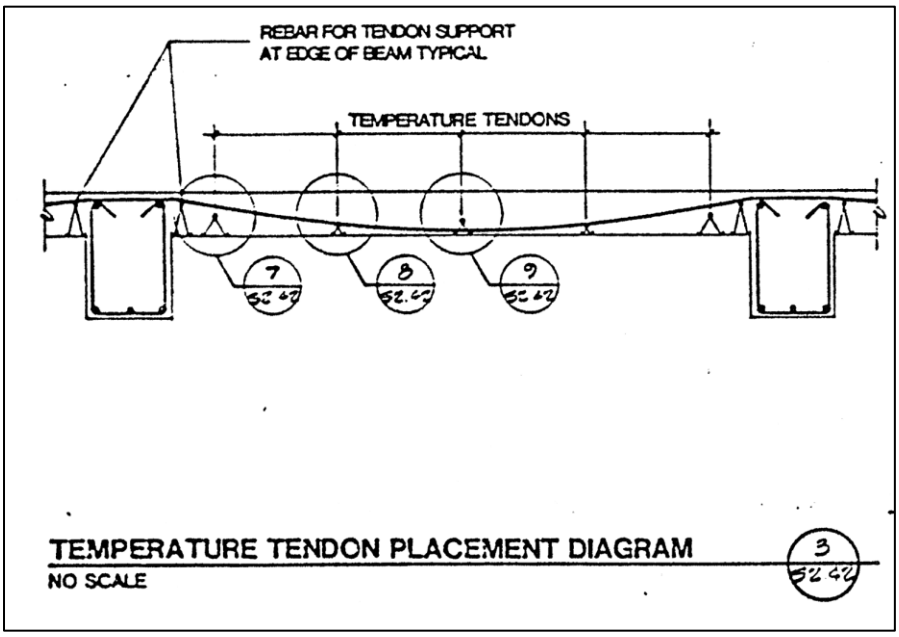

Figure 1-9 Schematic of the post-tension cable sag running through the slab between beam supports, from the as-built 1988 structural drawings.

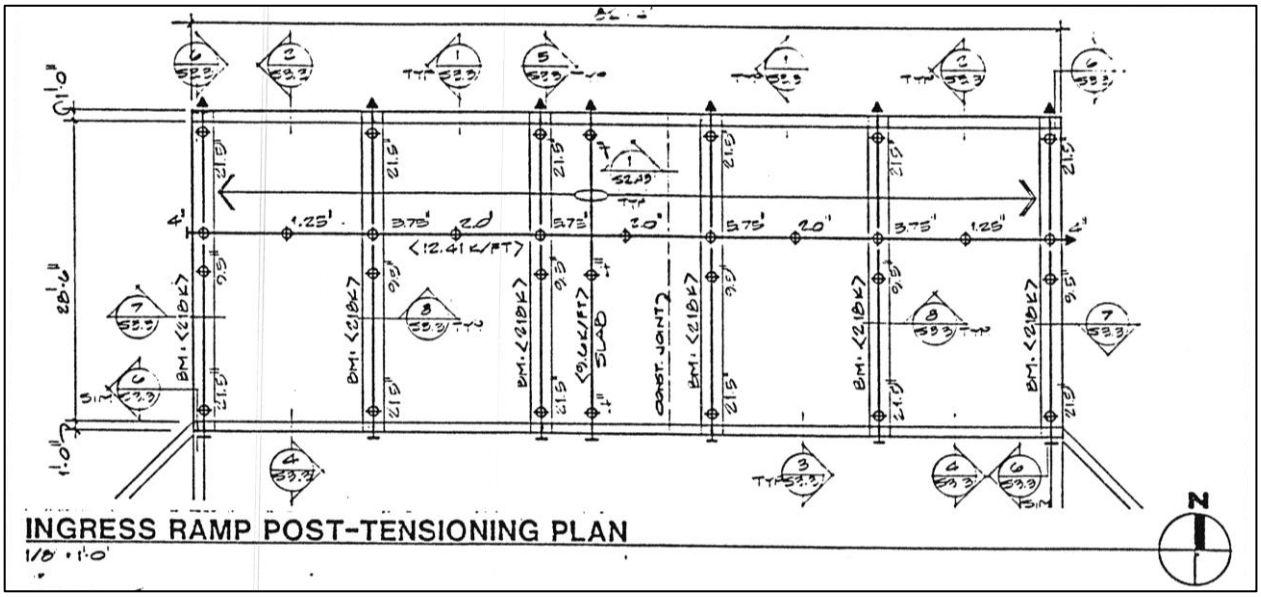

Figure 1-10 Example of the as-built 1988 structural drawings showing the post-tensioning in the entrance ("ingress") bridge from the ingress ramp to the first floor of the garage.

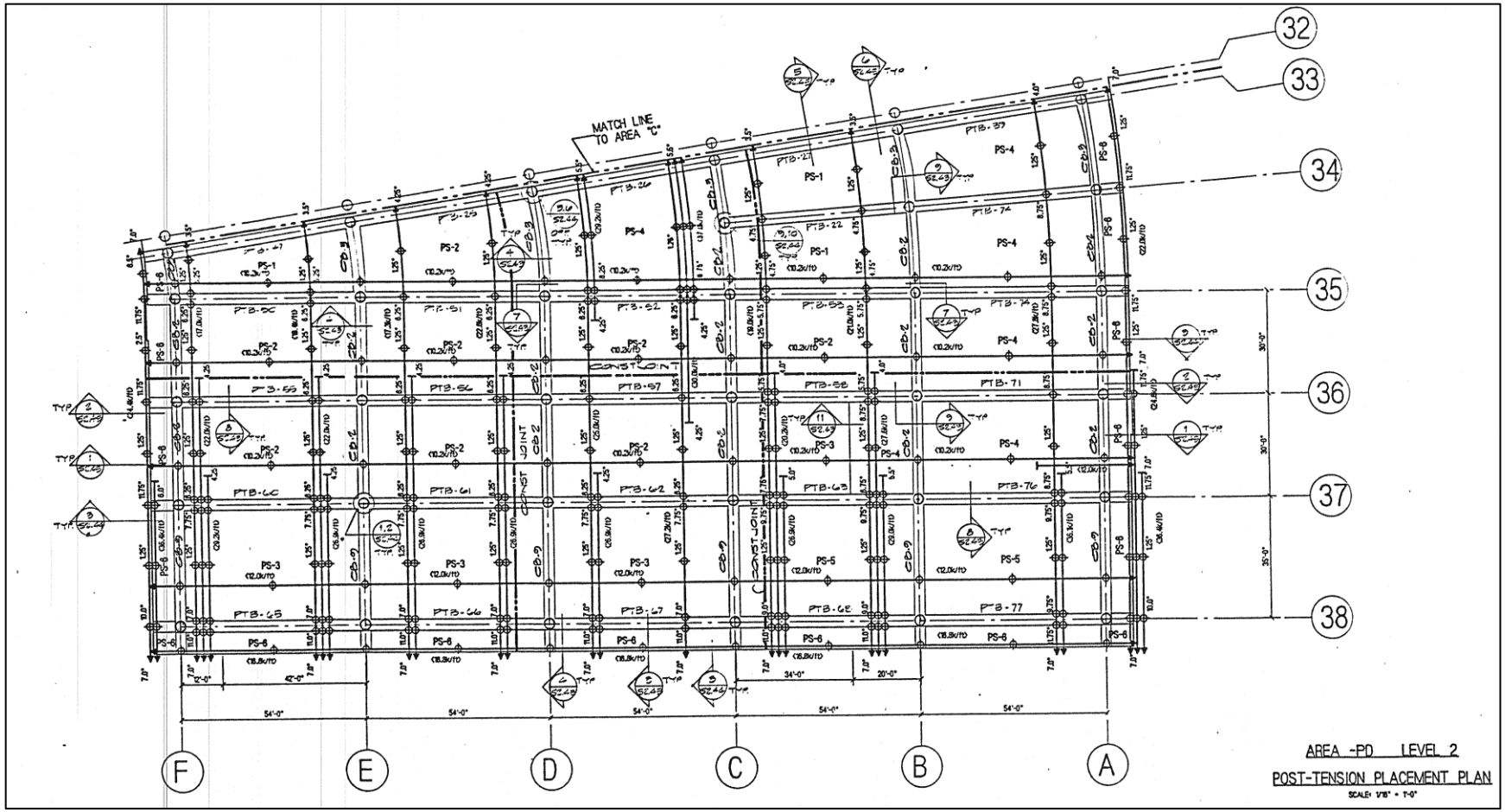

Figure 1-11 Example of the as-built structural drawings from 1988 showing the first floor ("level 2" on drawing) post-tensioning reinforcement system in structure D (the southeast corner).

The helix structure slabs were 8 inches thick with No. 4 epoxy-coated rebar at 16 inches on center and PT cables radially across the driving loop. An example of the layout of the reinforcement for the helix structure can be seen in Figure 1-12.

The entrance SOG ramp leading up to the entrance bridge was reinforced with No. 7 epoxy-coated bars at 12 inches on center each way. There was no reinforcement in the ground floor SOG.

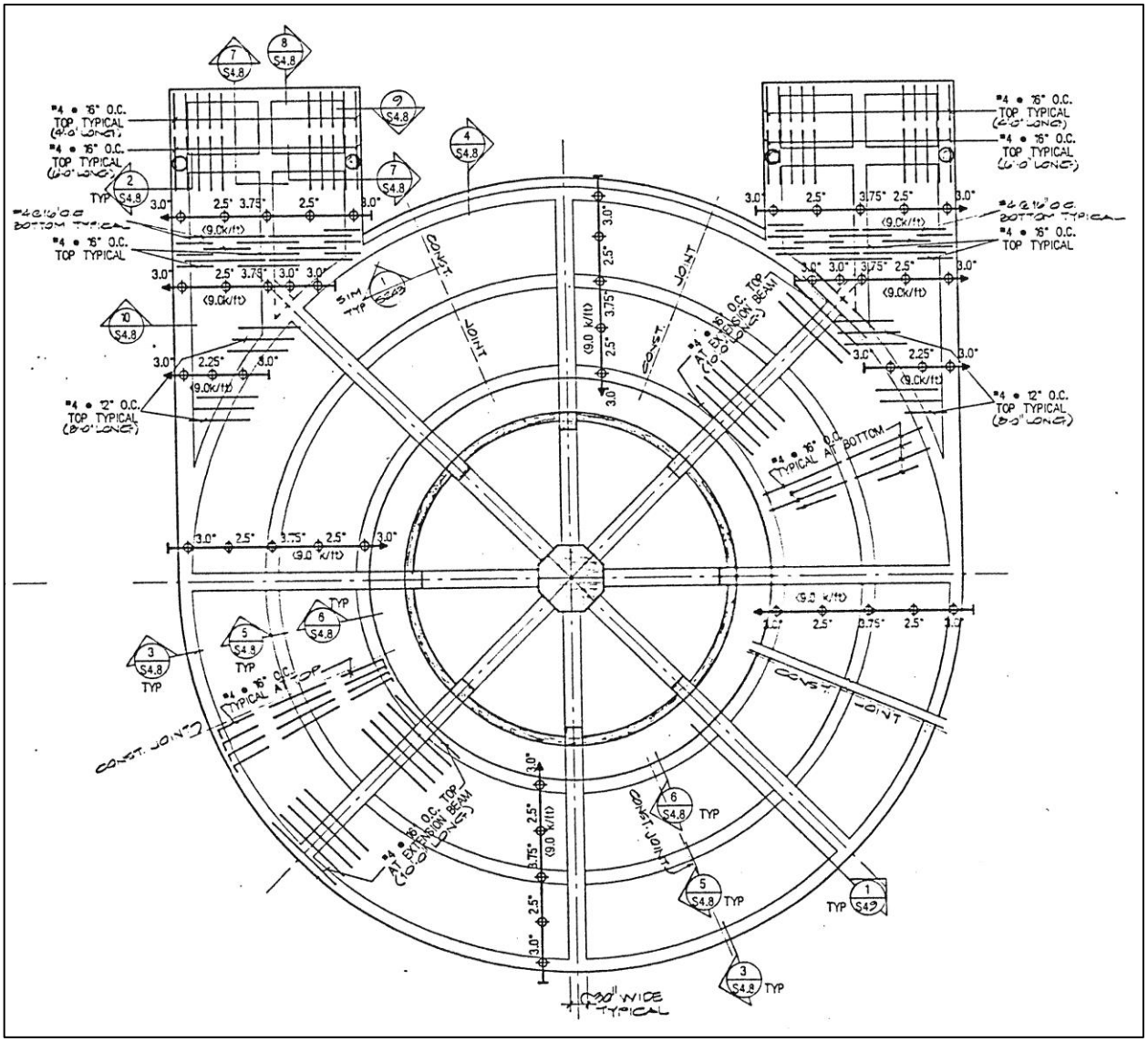

Figure 1-12 Example of the as-built 1988 structural drawings showing the post-tensioning and epoxy reinforcement in the up-helix ramp from second to third floor.

1.2.4 Mixture

The parking garage was unique in using a silica micro-slurry, a relatively new supplementary cementitious material (SCM) at the time of construction. Based on a recent meeting to recall the history of the structure, it was noted that the use of the micro-silica would increase the cost of the structure by one million dollars. The added cost of the specific silica additive was originally declined by the airport, but after further investigation of airports in Kansas City and Cincinnati that used micro-silica, the airport officials decided the benefits would pay off. Originally the structural details required 7.4% silica fume and 15% fly ash, by mass of cementitious to be used. Anecdotally, the concrete supplier, Geneva Rock, reported that after mixing trial batches, they settled on a 9% micro-silica slurry, 0% fly ash mixture to achieve the rapid chloride permeability testing (RCPT) requirement. The authors presumed that the 9% by weight cementitious replacement of micro-silica was pre-mixed with the batch water to create the slurry.

The structural drawings specified the strength of the elevated slabs to be 6 ksi, and the slab-on-grade to be 4 ksi at 28 days. The suspended slabs, bridge, and helixes were all made with concrete containing the silica fume additive. All the SOG sections (ground floor) were constructed using plain concrete containing no SCMs. The w/c ratio of the final mixture was noted to be 0.38 (for all elevated and SOG sections), had 6.5 bags of cement per cubic yard, and a 7% (+/- 1%) air content. The cement supplier was Holnam (now Lafarge-Holcim) located in Morgan, UT and made a finer ground Type II cement especially for the project to increase the concrete strength. The aggregate blending was customized to have a higher concentration of ½ inch size to decrease the permeability and had a low coarse-to-fine aggregate ratio of 0.38. The mixture also contained a

high range water reducer to improve workability for the use of the micro-silica, low water-cement ratio, smaller aggregate blend gradation sizes, and finer ground cement.

The concrete supplier, Geneva Rock, batched the concrete in 8 cubic yard loads at the time and a three-conveyor system was used to reduce air loss instead of pumping. Since the micro-silica slurry was significantly different and difficult to finish, the installers were required to attend training sessions on finishing and curing. The concrete slabs were poured at night in narrow strips and finished by bull-floating and brooming. The helix ramps were finished with a rake to cause a grooved concrete to fold over. There was no bleed water on the surface. The concrete was wet cured for some unknown duration of time.

The testing firm, PSI, cast several 6-inch cylinders at the same time as the garage construction. These were reported to be placed on the deck and covered with a blanket to simulate the field curing on the actual slab. Cylinders were tested every hour to plot the strength gain versus time. This helped in predicting when the concrete would reach its desired strength for applying the post-tensioning stress. Anecdotally, the testing firm noted that by 28 days the concrete was stronger than their loading apparatus could handle (>10.6 ksi). A single cylinder of the construction concrete was saved and tested at the University of Utah's lab after 28 days. It was found to also exceed the strength of the machine at over 15 ksi.

1.2.5 Loading, Traffic, and Environment

The structural design indicated that the PT cables could be tensioned when the concrete reached 4.5 ksi. The structure was stressed in stages to reduce cracking. When the concrete reached 50% of its required strength, 50% of the PT stress was applied. When it reached its full strength, 100% of the PT stress was applied. Anecdotally, the SLC Airport personnel indicated

that any cracks that appeared prior to the garage's opening in 1991 were sealed with epoxy resin by the contractor.

The parking garage was designed to handle a seismic load since the SLC area is prone to earthquakes. Since the time of its construction, the largest nearby earthquakes (Earthquake Track 2020) were,

- 4.7 magnitude in Nephi, UT (88 miles away) in April 2003,
- 6.2 magnitude in Wells, NV (186 miles away) in February 2008,
- 4.6 magnitude in Randolph, UT (104 miles away) in April 2010,
- 4.6 magnitude in Junction, UT (211 miles away) in January 2011,
- 5.3 magnitude in Soda Springs, ID (161 miles away) in September 2017, and
- 5.7 magnitude in Magna, UT (16 miles away) occurring in March 2020.

There was no noted damage observed from any of these earthquake events.

The parking garage's suspended layers had a ticketed entry and exit system which allowed the airport personnel to know how many vehicles were in the structure at a given time. Though it is not known specifically where in the structure the vehicles parked, some general trends were noted. When the structure was first constructed, there were six lanes on the entrance ramp (before the ticket booth), and four driving lanes between columns A-B of which two continued for the economy lot parking. In this original design, vehicles intending to park for the short-term (hourly or daily parking rates) could use the three entry ticket booths that brought them into the driving lane between columns B-C. In subsequent years, the layout was modified such that two of the lanes between columns A-B were converted to diagonal parking stalls.

According to the as-built architectural drawings, the capacity of paid parking stalls (those on the suspended slabs) was 1,854. Sunday through Friday the garage would fill close to full capacity. Tuesday through Thursday between 9am to 2pm the garage would close because it hit capacity. Saturdays the garage would reach 50% capacity. Very few cars would stay for more than one day in the lot. Data provided from the SLC airport indicated that in 2019 alone, 938,180

vehicles passed through the garage. This was more than the 843,135 vehicles that passed through the nearby, uncovered economy lot. See Figure 1-13 for the monthly distribution. The ground floor was used for rental cars and its traffic flow was not tracked by the airport.

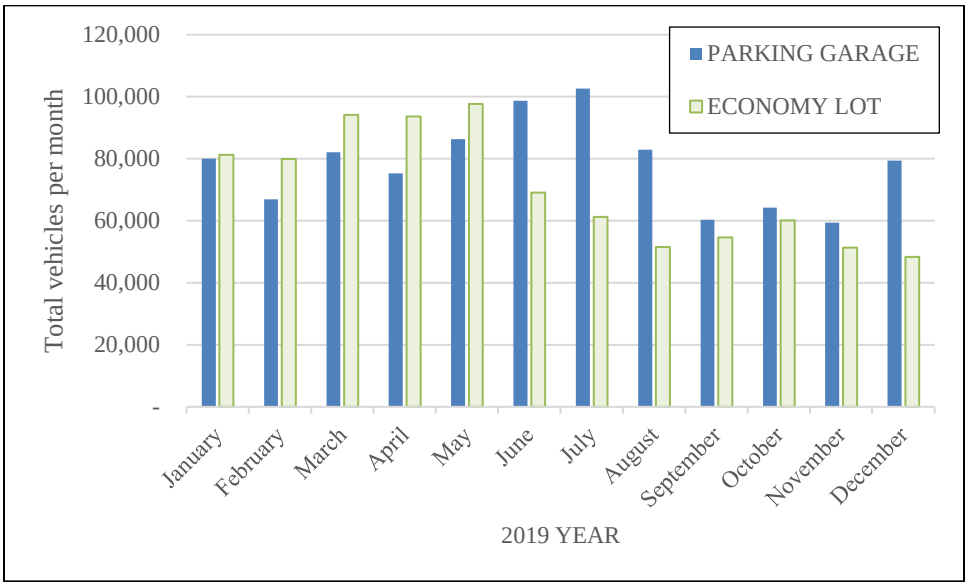

Figure 1-13 2019 monthly traffic volumes in the parking garage and economy lot at the SLC Airport.

In the parking garage, most vehicles would park closest to the concourse bridges leading to the airport terminals. These were located on the north side of the structure either between columns 28-29 or by column 14. Most vehicles parked on the first floor. The second and third floors were last to fill on busy days or contained airport staff.

Since it was outdoors, the parking garage was subject to freeze-thaw cycles. The sidewalls on the exterior would have reduced the amount of wind gusts on the slab surfaces. Compared to other states, Utah has an arid climate most days of the year which reduces corrosion. Most likely, the SLC Airport applied salt to the surrounding terminal road and the parking garage entrance ramp. It is expected the highest salt exposure will be on the entrance ramp, bridge, and possibly

the first suspended floor. The specific type of salt used or dosage rate of salt applied was not recorded. It was stated that two times a year the maintenance crew at SLC airport power-washed the garage's concrete slabs to remove the salt.

1.2.6 Joints and Maintenance

Each suspended floor was poured into 30 slabs. The bridge deck was poured into one, continuous slab. Slab seams were sealed with epoxy on all suspended slabs. The ground floor had unsealed saw-cut joints for the slab-on-ground. Construction joints were located across the structure at a third of the span or where the PT was at its center of gravity for the slab. These construction joints had two keyways, each were 2 inches deep, 4 inches tall and sealed with an epoxy resin.

The airport personnel noted that no maintenance or additional sealing of joints or cracks was performed throughout the subsequent service life of the garage. It is thus presumed that any sealed cracks appeared during the construction of the parking garage. These cracks, though sealed, may still have opened and closed during loading and freeze-thaw cycles during the garage's service life.

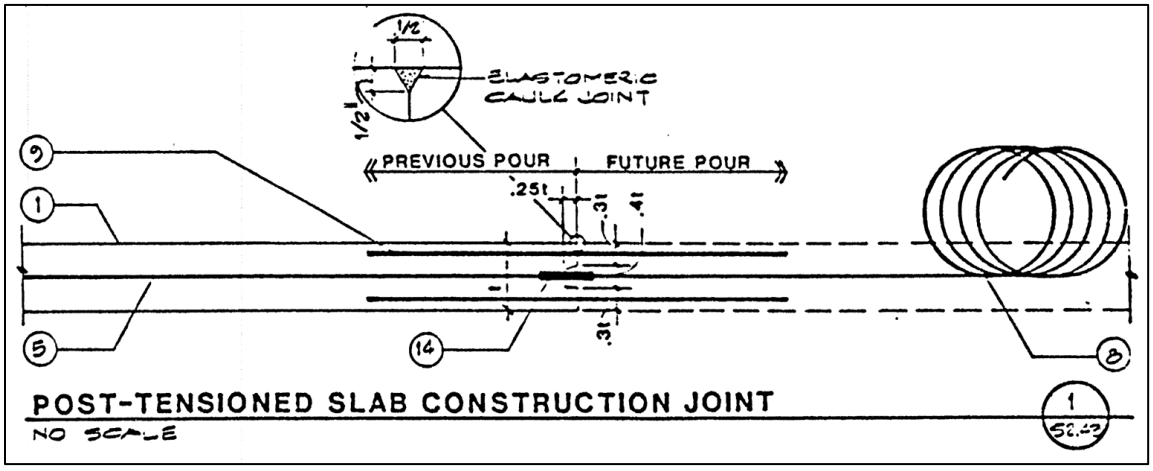

Figure 1-14 Schematic of the post-tensioning continuing through a construction joint in a slab, according to the as-built 1988 structural drawings.

1.3 Literature Review

1.3.1 Silica Fume Use

Silica fume is a by-product of silicon created from silica (quartz) and carbon (coal, coke, and wood chips). When heated, silica and carbon mix and release silicon gas. This gas reacts with oxygen and creates silica fume powder.

Around 1950, scientists discovered that silica fume was beneficial to concrete. Around 1950, silicon factories were no longer allowed to dispose of silica fume into the air. They started filtering it, and in 1980 started selling it to concrete companies. Ever since then, the concrete industry has used silica fume to increase concrete's performance (Fidjestøl and Dåstøl, 2008).

Low permeability concrete reduces chloride penetration rates which reduces the money spent to replace or fix corroding reinforcing steel. When added to concrete, silica fume reduces the concrete's pore size which reduces chloride penetration.

1.3.2 Epoxy Reinforcement Bars

Coating the outside layer of steel reinforcement in epoxy creates a corrosion protectant for the steel once inside the concrete. The epoxy coating shields the steel from corrosive materials and is supposed to maintain the integrity of the steel throughout the structure's life span. Epoxy-coated rebar was first used in 1973 on a bridge in Pennsylvania. By 2013 it was used in about 80,000 structures in the U.S. and Canada (Epoxy Interest Group n.d.).

At the time the garage was built, epoxy-coated rebar was also used with the intention to reduce corrosion rates in reinforcing steel. #4 and #7 epoxy-coated reinforcement bar were used in the SLC airport parking structure along with coated tie wires to further enhance corrosion protection.

Since then, epoxy-coated rebar has been further studied and tested. Studies in the U.S. and Canada have shown that epoxy coating can cause pitting corrosion. When the coating is scraped or nicked during placement and handling, the rebar is exposed to chlorides. Instead of uniformly corroding the rebar, the corrosion is concentrated and accelerated at the nick. This can cause the rebar to suddenly break due to the weak spot at the nick (Ley, 2018).

1.3.3 Post-Tensioning

PT members were first developed and used in the 1950s. In the 1980s people began to use them in lower-level parking garages of high-rise buildings. In the 2000s it became regular practice to use them in skyscrapers and other concrete structures.

While rebar has a yield strength of 60 ksi, PT tendons have an ultimate tensile strength of 270 ksi. They greatly increase a concrete slab's tensile strength while also reducing construction and material costs. PT-reinforced slabs can be designed to be thinner since they add so much strength to a slab. This reduces the concrete material weight and cost for a structure (Khosa, 2019).

1.3.4 Comparison with Other Bridge Decks and Parking Garages in the United States

In 2001 and 2002, core samples were taken from four bridge decks built with silica fume concrete in New York and Ohio. The cores were tested at the University of Toronto to determine their chloride content and diffusion coefficient. Hooton et al. discovered that the silica fume concrete decks have bulk diffusion coefficients ten times lower than non-silica fume concrete as well as a much lower average of coulomb values indicating lower levels of chloride penetration (Hooton et al., 2010).

In Appendix A, Table A-1 shows the difference in crack density between different bridge deck structures of different concrete and reinforcing types. The bridges are located in the United

States, in Utah or states similar to Utah in their freeze-thaw patterns. The bridges varied in age from two to nine years old when cracks were analyzed, and found to exhibit crack densities ranging from 0.046 ft/ft^2 to 0.36 ft/ft^2.

The crack densities of the bridges are much higher than that of parking garages. Inspection reports of parking garages in the United States are not often reported in the literature likely due to the ownership being more private than the public government ownership that most bridge decks are. It was estimated that in California parking garages up to three levels high, only 0.009 ft/ft^2 of cracks would need to be repaired during the design life of the structures (Aalami and Barth, 1989). Factors leading to lower cracking rates in parking garages are expected due to different geometry (two-way slabs with varying spans and shapes), loading type (smaller vehicles instead of heavy-loaded semi-truck trailers), reinforcement (some PT reinforced), curing method (structure closed until completed, so easier and longer cures), and climate exposure (covered or some wind protection).

2.0 DATA COLLECTION

2.1 Overview

The UVU and BYU teams performed visual inspections and physical tests on the parking garage. The tests and standards followed can be seen in Table 2-1.

Table 2-1 Methods Used to Collect Data and Samples at SLC Airport Parking Garage

Data Collected	Method for Collecting Data	Number of Replicates/ Location	Standard
Crack Density of Structure	Crack Mapping/AutoCAD	NA	None
Strength of Concrete	Schmidt Hammer Test	10 readings per grid point	ASTM C805
Debonding Locations	Chain Drag	NA	None
Rebar and Post-Tension Steel Locations	Pachometer Scanning	2 readings per grid point	None
	Ground Penetrating Radar (GPR)	Rolling scan	None
Concrete Cover Quality and Presence of Epoxy Coating on Rebar	Vertical Electrical Impedance (VEI)	1 point per grid point or rolling scan	None
Chloride Content	Drilling and Dust Collecting	1 - 2 drill holes per core	ASTM C1152
Chloride Permeability	Cores	3 - 6 cores per sampling location	ASTM C1202, ASTM C1556

The machine used to perform the VEI was invented by BYU. So far, there is no standard for using it. The machine can be seen in Figure 2-1. The machine sprayed water onto the concrete to increase electrical conductivity at the concrete's surface. The machine measured the concrete's reinforcing steel's degree of protection. The crack mapping, VEI, and Pachometer tests were used by UVU and BYU to choose drilling and coring locations.

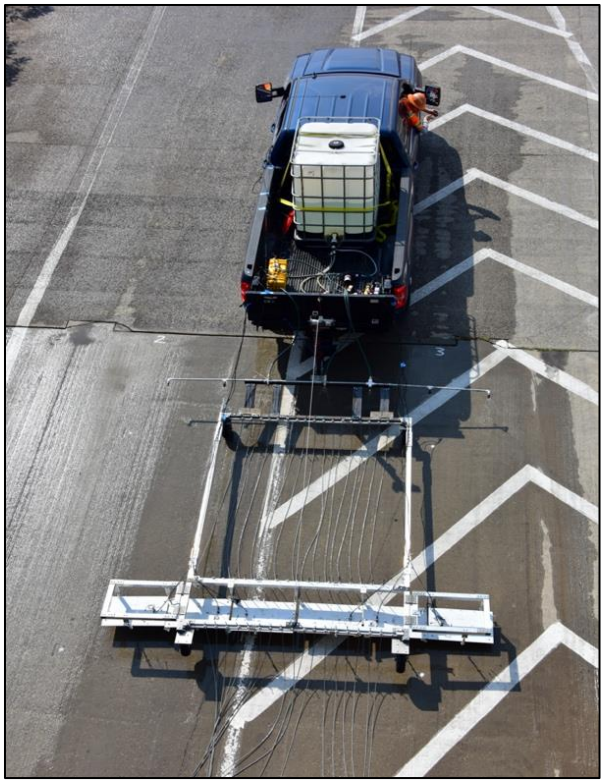

Figure 2-1 Vertical Electrical Impedance machine, invented by Brigham Young University, on the bridge deck of the SLC airport parking garage.

2.2 Data Collection Strategy

The purpose of the data collection was to determine how the silica fume and plain concrete properties compare across the entire garage. Five locations in the whole parking garage were selected. One from each floor and one from a helix. These five locations were:

- Ground floor (unreinforced, plain concrete)
- First floor entrance bridge (epoxy-coated rebar and post-tensioned cables, silica fume concrete)
- Second floor, south end (epoxy-coated rebar and post-tensioned cables, silica fume concrete)

- Third floor, west end (epoxy-coated rebar and post-tensioned cables, silica fume concrete)
- Helix up ramp (epoxy-coated rebar and post-tensioned cables, silica fume concrete)

A grid was spray painted onto the concrete at each flat slab location, similar to that shown in Figure 2-2. The entrance bridge was divided into 6 lanes instead of a rectangular grid pattern. The helix ramp did not have a grid placed down, instead one data set was collected per level. Data and samples were collected on clear days with no rain.

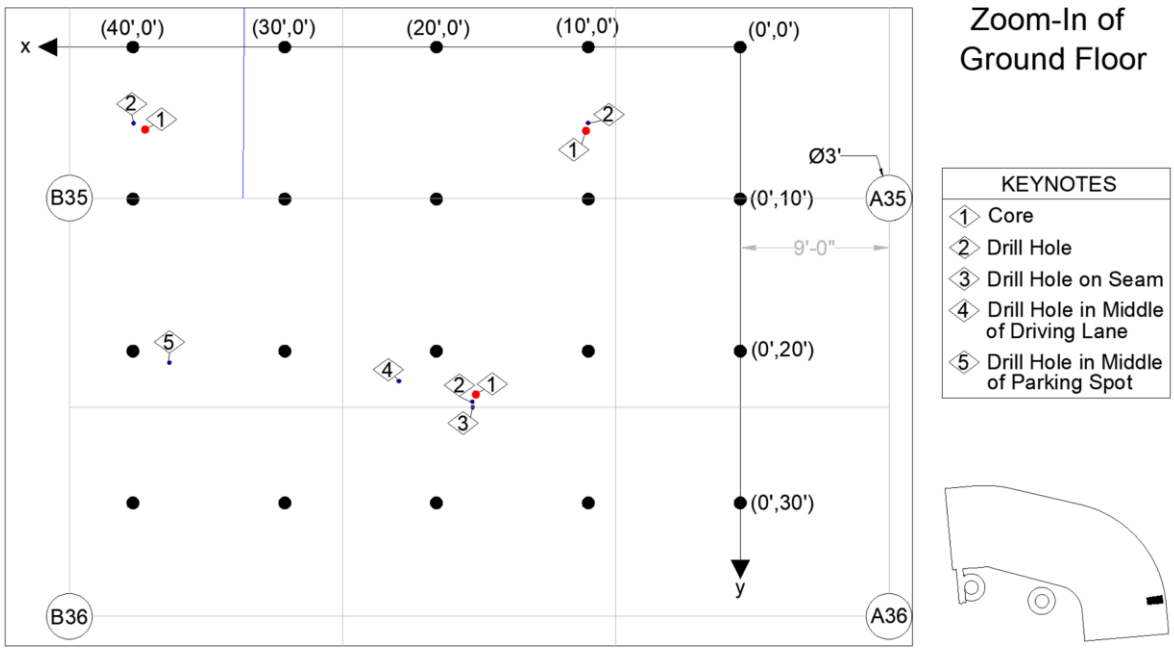

Figure 2-2 Zoomed-in view of data sampling area taken on the plain unreinforced concrete on the ground floor. The black dots were for Schmidt hammer readings; red dots for core sample locations; blue dots for chloride drilled sample locations; gray lines were saw-cut joints; and top-down cracking (blue line).

In general, on all of the suspended floors, at least three location sets of powder-drilled samples were taken for chloride analysis. Of each location set, one sample was obtained on a crack (note: all suspended slabs had epoxy-filled cracks), and the other sample was obtained four inches away from the crack. If there were no cracks within the grid location, samples were randomly taken. For the entrance bridge laid out in lanes, powder-drilled samples were obtained

at least from each lane, again on a crack (these were unsealed on the bridge deck) and four inches away from a crack. On the ground floor, powder-drilled samples were taken from the middle of a parking spot, the middle of a driving lane, the wheel path of the same driving lane, and from the lowest and highest point within the grid's sloped floor gradient.

2.3 Cracking

Concrete cracking locations indicate weak spots or areas that underwent high amounts of tensile stress at some time after placement. In general, cracking is expected to be seen in all structures, but expected to be reduced in post-tensioned structures if compared to the same design without the post-tensioning. Since a side-by-side comparison was not available, mapping the cracks found in the structure provides some insight into where stresses may have been unusually high from mechanical loading, environmental stress, or from chemical attack to the concrete or reinforcement. For this particular parking garage structure, most of the cracks were observed to be epoxy-sealed, and since sealing of the cracks was performed early on by the original construction contractors, the authors anticipated most of the cracking was caused my early pre-loading or chemical shrinkage occurrences. These cracks, though sealed, may accelerate the degradation of the reinforcement by allowing shorter paths for water and chlorides to reach reinforcement.

2.3.1 Surface Observations and Delaminations

The concrete slab surfaces were rough but remained intact from the broom and rake finishing on the levels and helix structures. There were a few locations on top of the suspended

floor slabs where the reinforcement was exposed, and the concrete cover spalled off. There were also a few spalling locations seen on the underside of the northwest downward helix ramp.

The chain-drag technique was used to audibly identify potential delaminations in the structure. This was performed on all suspended slabs and the helices. Only one location of audible delamination was found with the chain drag, a 3-inch diameter spot on the first floor close to the terminal entrance in structure C. There was no visible spalling at this one delamination site. No other audible delamination was found in the entire structure.

2.3.2 Visual Observations Recorded

Three types of visual analysis were done in the parking structure: the width of cracks, the location of cracks, and presence of efflorescence. A typical crack and crack width is shown in Figure 2-3. As stated previously, almost all floor cracks on the suspended slabs were filled with an epoxy. The cracks observed in the bridge deck were not sealed. The sidewalk added to the edge of the suspended slabs was not analyzed for the crack density study, but there were some wide cracks observed on some of these, as shown in Figure 2-4a. The helix structure had some sealed and some unsealed cracks. Also mentioned previously, there were a few locations where the rebar was exposed, an example image of this is shown in Figure 2-4b. The yellow color is likely due to the dry rust or debris that temporarily is covering the reinforcement. An example of the efflorescence found is shown in Figure 2-5. As a general observation, efflorescence was found on or near almost every visible ceiling crack, and was very abundant on each of the construction epoxy-filled keyway joints. Important to note was there was no exposed rebar nor red rust color found from the underside of slabs. From looking at the crack maps shown in section 3.2, top-down cracking was more commonly found near the corners and along the edges of the construction joints.

(a) **(b)**

Figure 2-3 (a) Typical epoxy-filled crack found on suspended levels of parking garage and (b) unsealed surface cracking on the 1st level in structure B with a 0.75mm width.

(a) **(b)**

Figure 2-4 (a) Wide floor crack found on the sidewalk on the southeast corner of the 1st level structure D, near the entrance ramp and (b) spalling and exposed rebar near the surface on the 1st level near northwest end of parking garage.

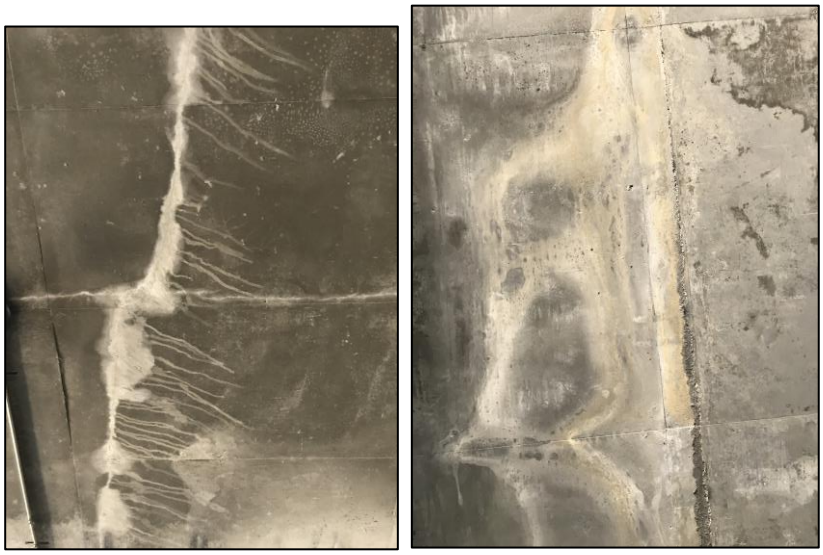

(a) (b)

Figure 2-5 (a) Ceiling efflorescence seen while standing on 1st level looking up at the 2nd level slab in structure C and (b) efflorescence around an epoxy-filled seam looking up from level two onto the bottom of the level three slab.

2.3.3 Calculation of Crack Density

The mapping of crack locations of the parking levels and helixes was obtained by visual inspection. General lengths and locations of cracks were measured using a measuring tape and were hand-drawn recorded on-site. Afterwards, the hand drawings were transferred to AutoCAD® where slab areas and crack lengths were used to calculate the crack density.

2.4 Summary

As of October 2020, all visual and physical samples and data have been collected from the parking garage. The data included in this report is the crack locations, crack densities, Schmidt hammer, and cover depth readings. Five locations or structure types were recorded from the

parking garage: two suspended parking slabs of silica fume concrete, a helix ramp of silica fume concrete, an onramp bridge deck of silica fume concrete, and an unreinforced non-silica fume concrete SOG.

3.0 VISUAL INSPECTION RESULTS

3.1 Overview

As previously described, one of the key results in this report is the crack mapping and density information. Additional data is shown here including the map of efflorescence and bottom-up visible cracks, the Schmidt hammer readings, and the cover meter readings.

The data collected through top-down crack mapping was used to calculate the total crack density. It was also used to determine which locations in the whole structure to lay out a grid for obtaining Schmidt hammer readings, cover meter readings, drilling samples, and coring samples.

3.2 Top-Down Crack Maps

The top-down crack maps are shown below in Figure 3-1 through Figure 3-5. The concrete slab construction joint seams (seen in gray) and top-down floor cracks (shown in blue) are plotted on these figures. In some locations, such as the top helix loops (from the third suspended slab to the roof) were not accessible due to a fence, and thus top-down cracks were not mapped.

As mentioned previously, many cracks in the suspended slabs appear to originate or connect perpendicular to the keyway construction joints. Since almost all of these cracks were epoxy filled, it is estimated that the top-down cracks shown most likely occurred very early, possibly within the first year, after the concrete was cast. The ground floor SOG had the least amount of cracking which is expected since it is an SOG, even without the reinforcement. Helices exhibited primarily radial cracking.

A few locations of exposed rebar were noted as shown in the figures for the 1st and 3rd floors and helices. These were rare, but appeared only in the west end of the parking garage or downward helix spiral.

The location of the two cores obtained in 2003 for the study reported for the Silica Fume Association (Hooton et al., 2010) were observed on the ground floor, as indicated in Figure 3-1. Any evidence of the remainder of the four other cores reported in this study, said to be from the 1st floor, were not found. It is unknown at this time why those core locations were not identified.

The suspended slab area with an observable higher crack density on the 2nd floor (between columns B-C and 37-38) was selected for further analysis with the grid point system. The VEI data (not shown in this report) indicated low impedance (meaning either low cover depth or significant internal cracking, defects, or rust) was identified on the top 3rd floor (between columns B-C and 1-2) even though there was no visible surface cracking there. The entrance bridge (1st floor) and ground floor were also selected for the grid-point system testing to see extremes in exposure (covered vs. uncovered), expected salt concentrations, material (silica fume vs. plain concrete), and reinforcement (epoxy + PT vs. unreinforced); but both entrance bridge and ground floor expected to have the highest traffic. The upwards (south/east) helix was selected instead of the downwards (north/west) for analysis primarily for safety reasons since, at the time, demolition had begun, and all parking garage traffic was channeled to use the downwards helix.

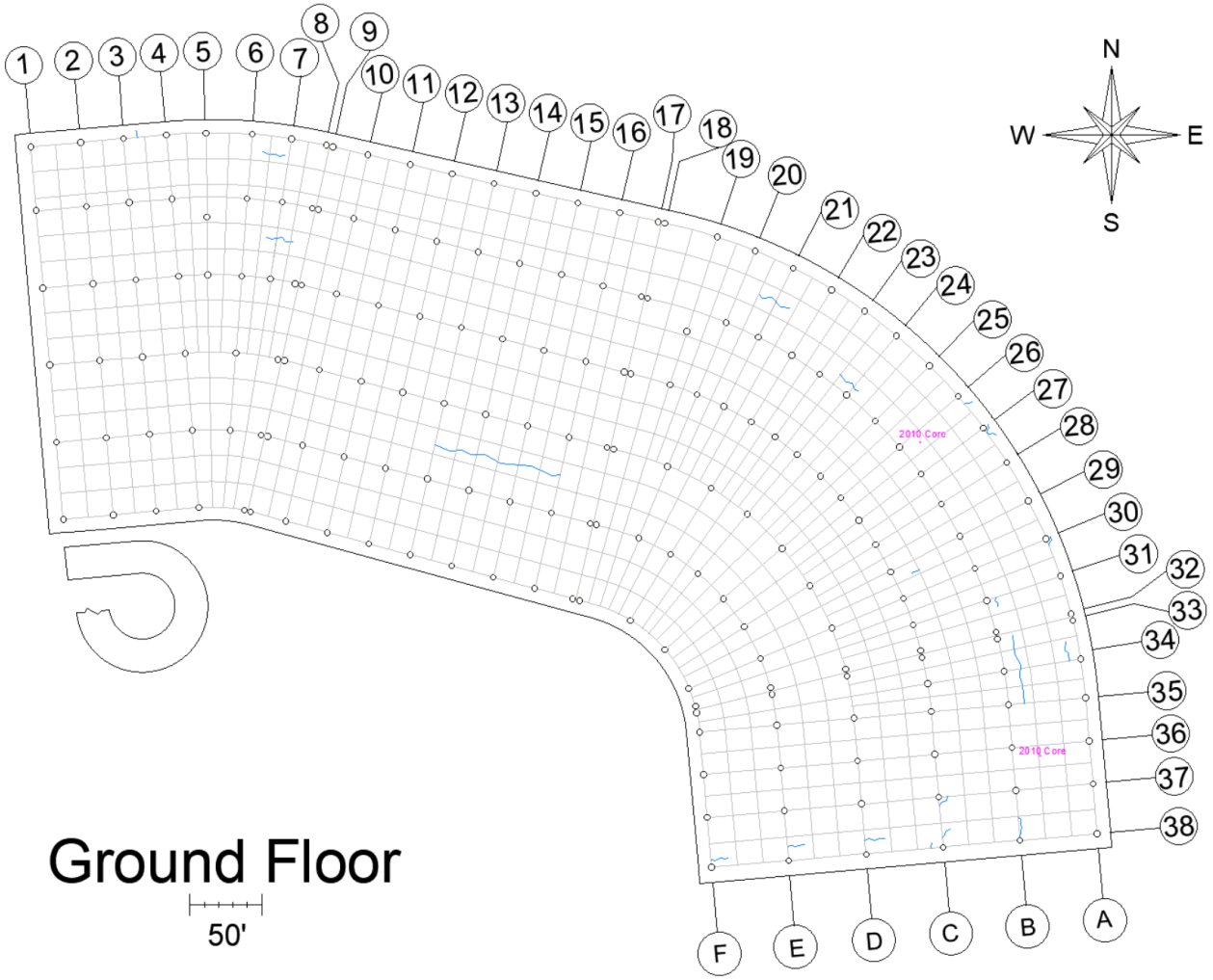

Figure 3-1 Crack map of plain concrete, unreinforced ground floor showing blue top-down cracks, gray saw-cut joints, and locations of the cores taken in 2010 study by Hooton et al. This floor was used only by rental car companies.

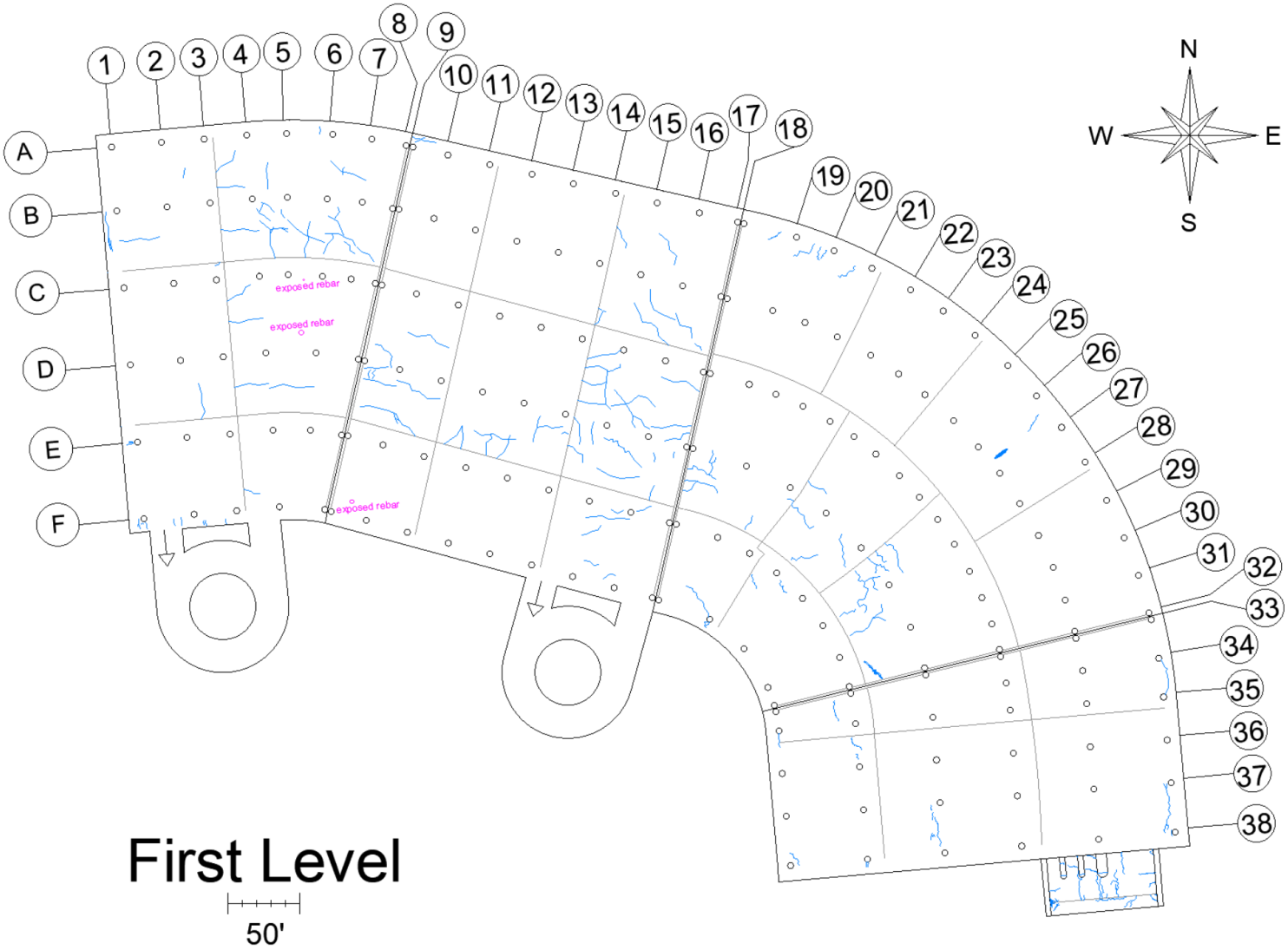

Figure 3-2 Crack map of silica fume concrete suspended, reinforced first floor and entrance bridge with blue top-down cracks, gray epoxy-filled construction joints, and locations of visually exposed rebar.

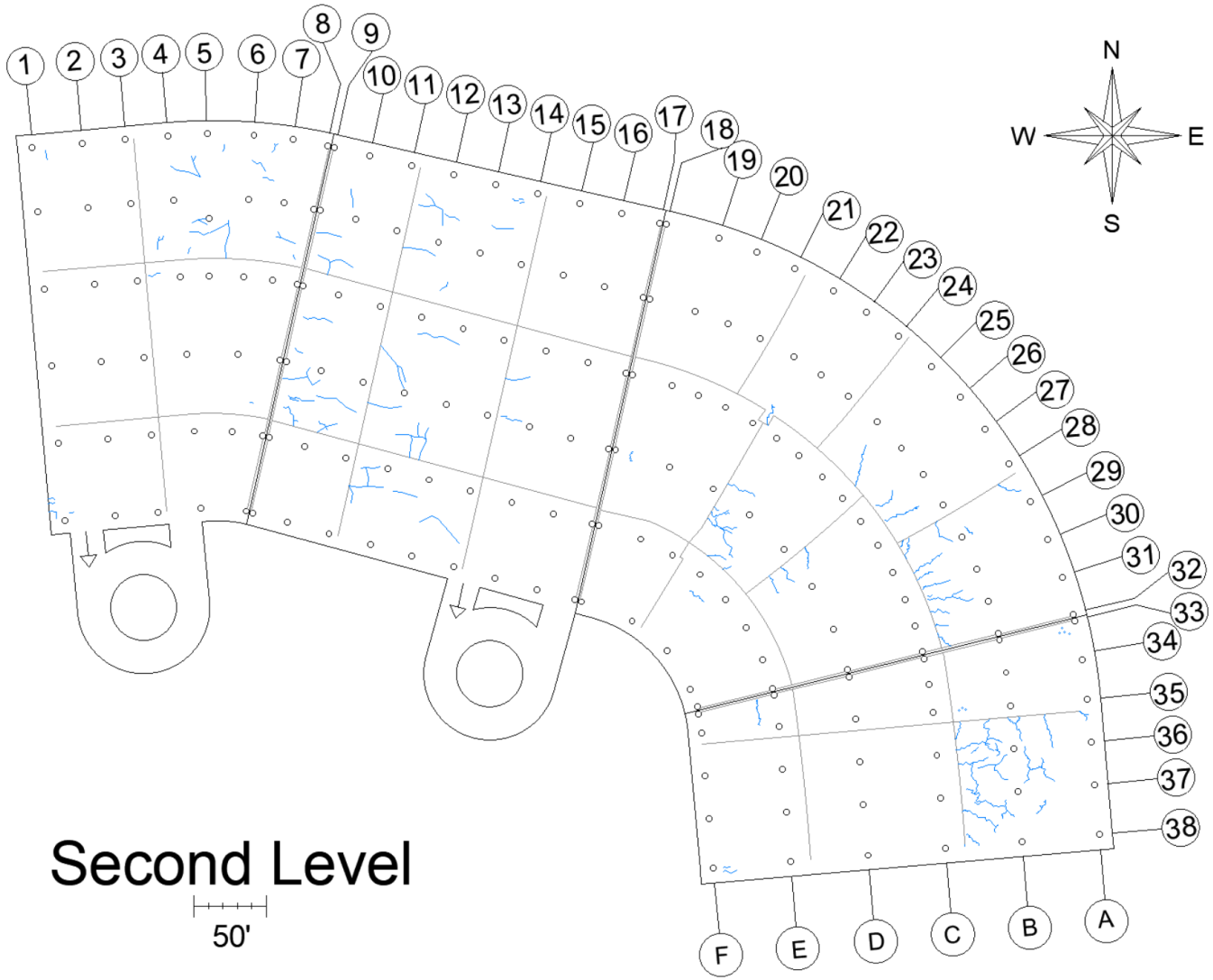

Figure 3-3 Crack map of silica fume concrete suspended, reinforced second floor with blue top-down cracks, gray epoxy-filled construction joints, and no locations of visually exposed rebar.

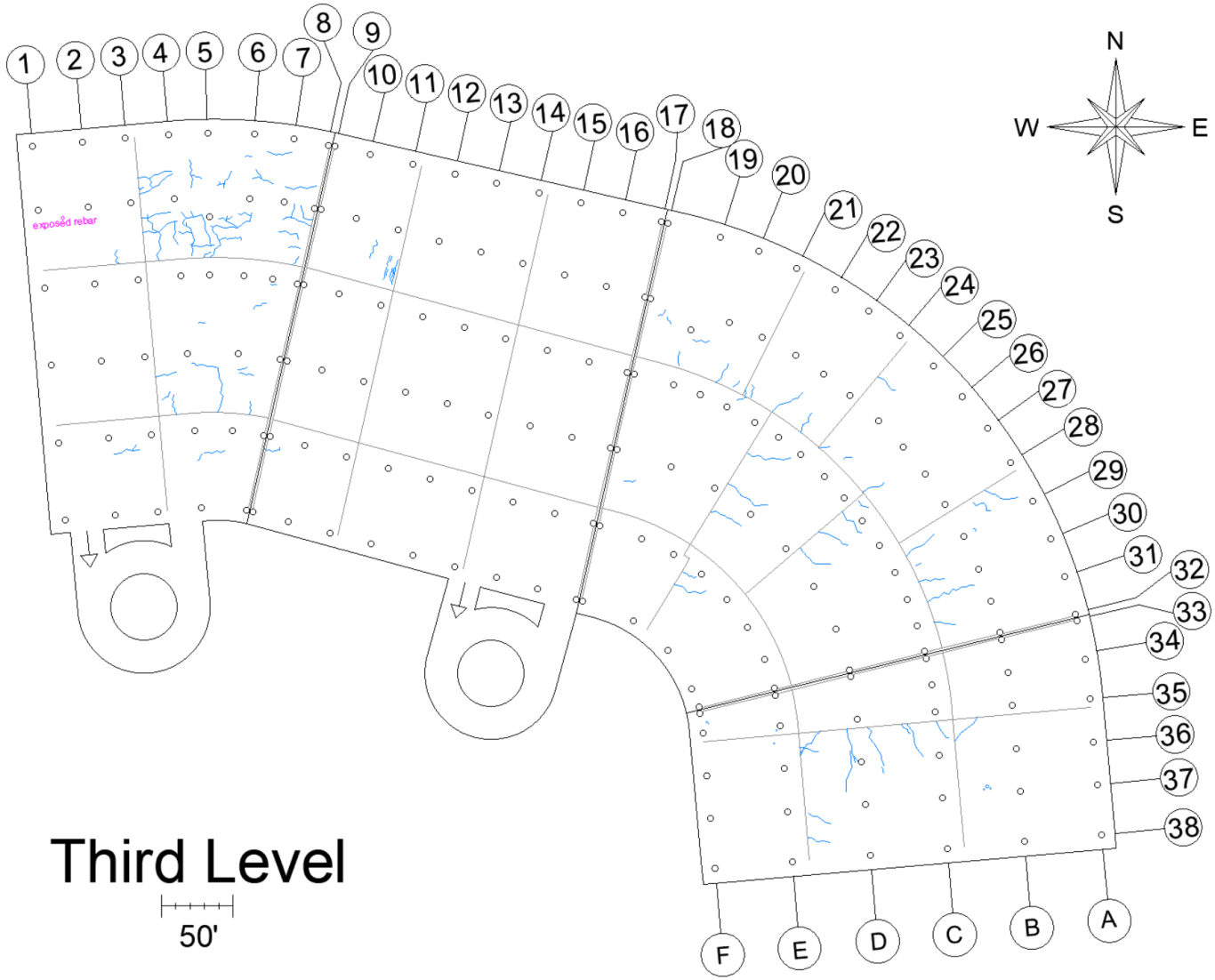

Figure 3-4 Crack map of silica fume concrete suspended, reinforced third (top) covered floor with blue top-down cracks, gray epoxy-filled construction joints, and location of a visually exposed rebar.

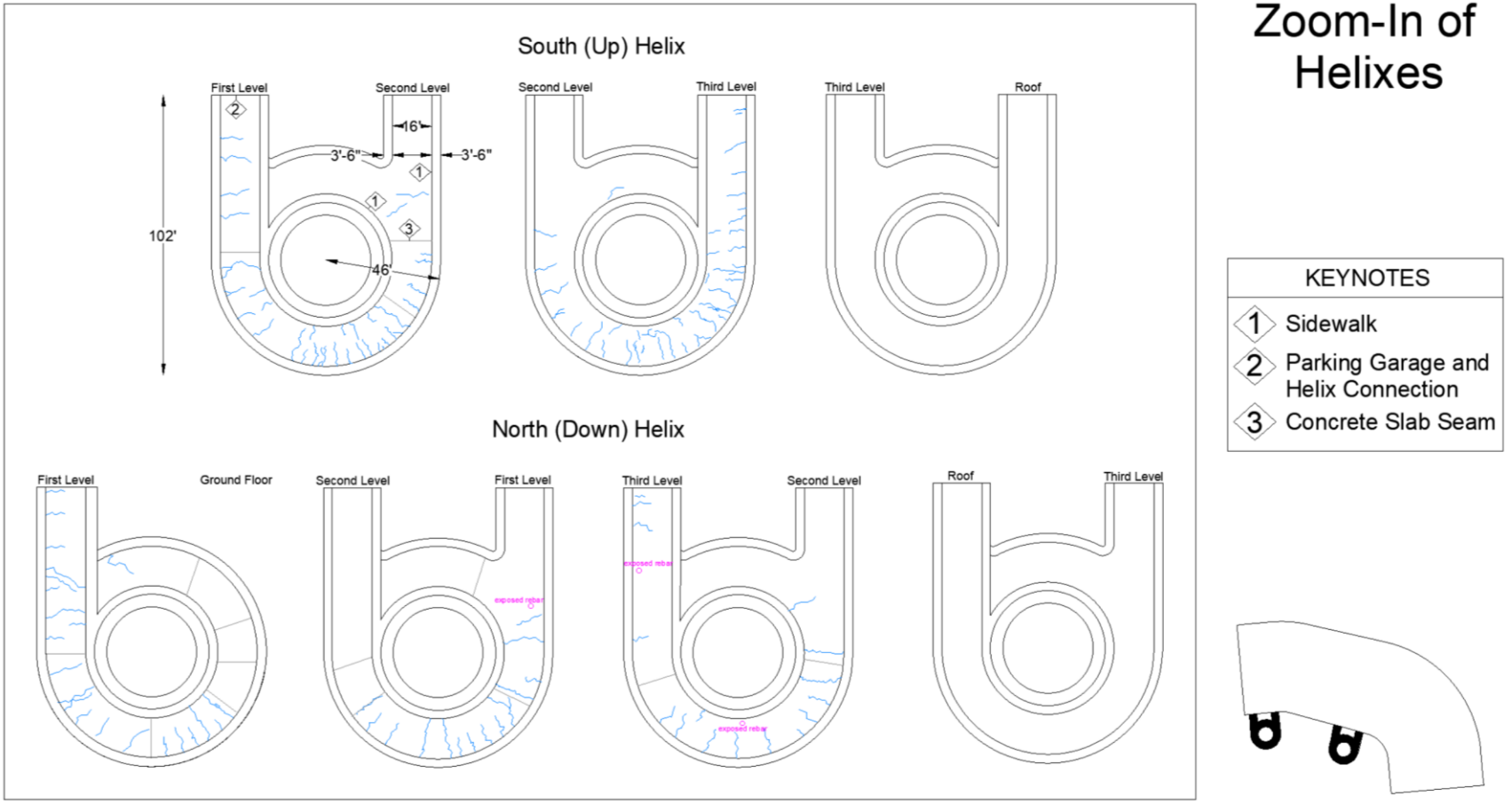

Figure 3-5 Crack maps of reinforced silica fume concrete helixes with blue top-down cracks, gray epoxy-filled construction joints, and locations of visually exposed rebar.

3.3 Bottom-Up Crack and Efflorescence Maps

Locations of bottom-up cracking and efflorescence were also mapped as seen in Figures 3-7 through 3-10. Some slabs that were on the ground (ground floor and first level of the helices) or blocked by construction barricades (entrance bridge) were not able to be mapped for their bottom-up or efflorescence locations.

As an overall observation, the helices appeared to have a significantly higher crack density (particularly in the radial direction) and a lot of efflorescence. Towards the center of the helix, stalactites ranging between one half and five inches were growing on the ceilings. Figure 3-6 shows efflorescence and stalactites on the ceiling of the southeast upward helix.

Several instances of exposed rebar were also present on the ceilings of the helixes. Where the rebar was exposed, there were large amounts of discolored efflorescence present suggesting rebar corrosion.

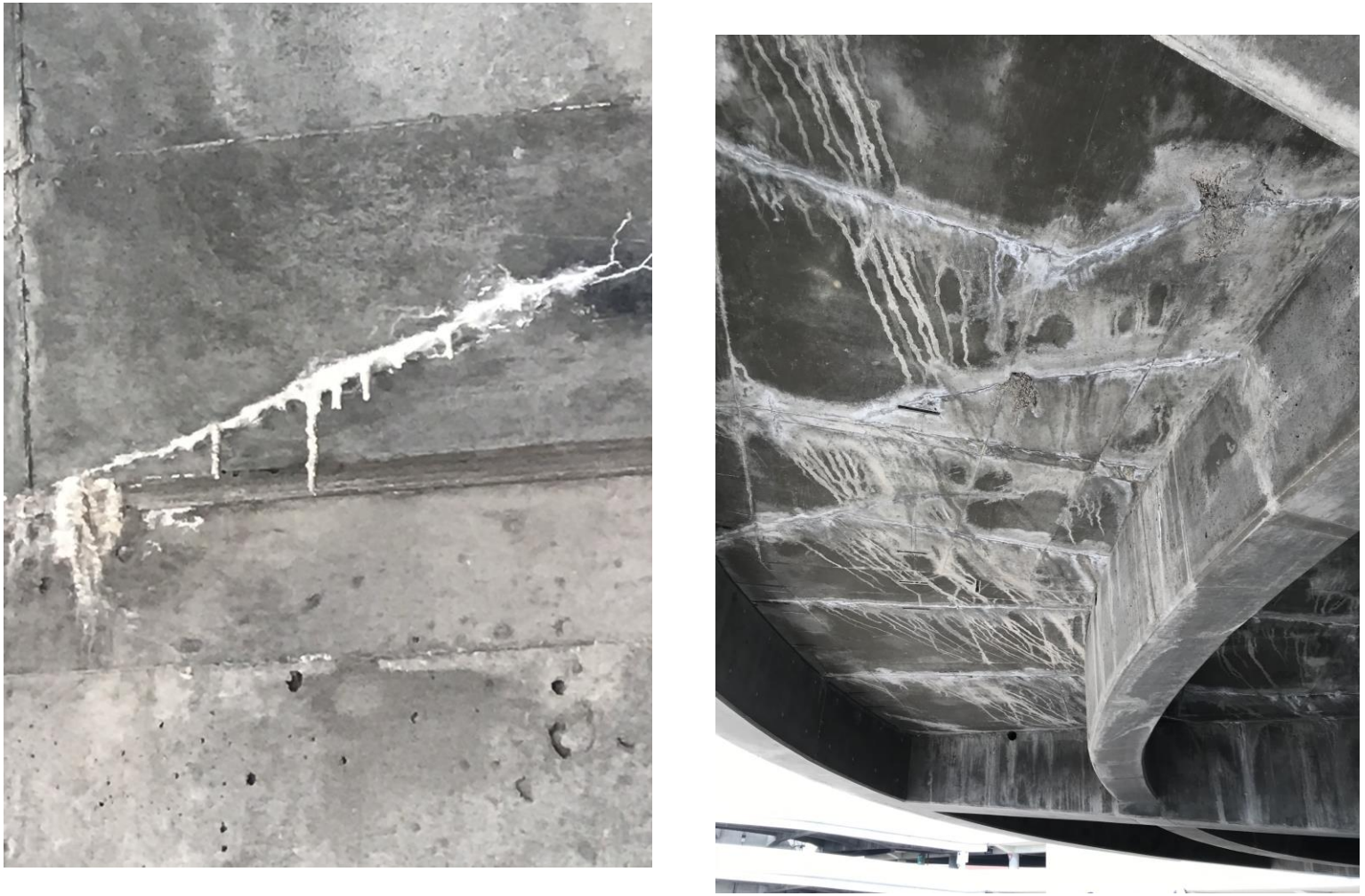

(a) **(b)**

Figure 3-6 (a) Photo of stalactites growing on the ceiling between first and second level on southeast helix, and (b) photo of the ceiling halfway between the first and second levels on the southeast helix. The efflorescence and cracking in this photo are similar to efflorescence and cracking on the ceilings of both helix structures.

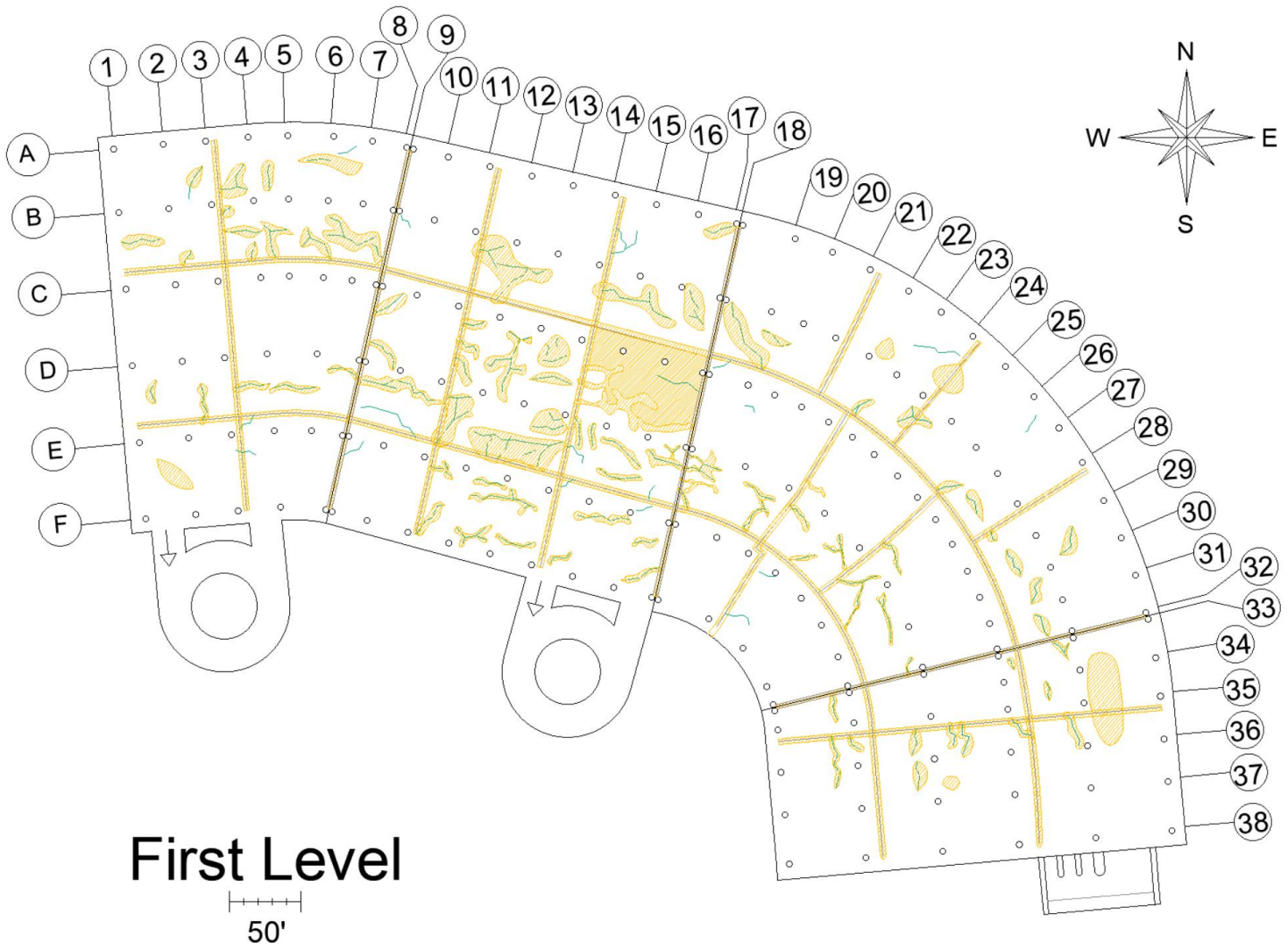

Figure 3-7 Crack map of the first suspended, reinforced silica fume concrete slab with green bottom-up cracks (some occurring along gray epoxy-filled construction joints) and yellow zones of efflorescence.

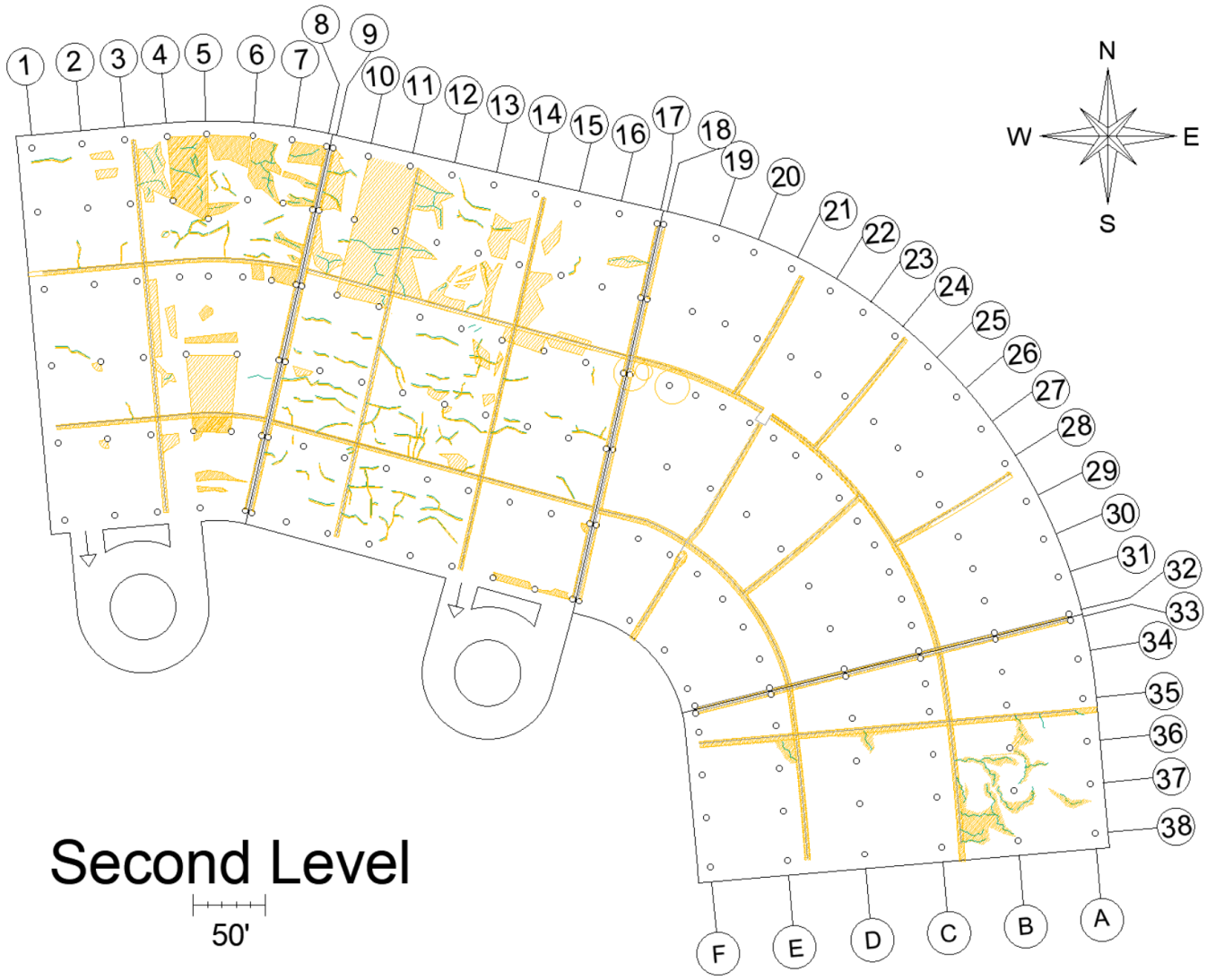

Figure 3-8 Crack map of the second suspended, reinforced silica fume concrete slab with green bottom-up cracks, yellow zones of efflorescence, and gray un-cracked epoxy-filled construction joints.

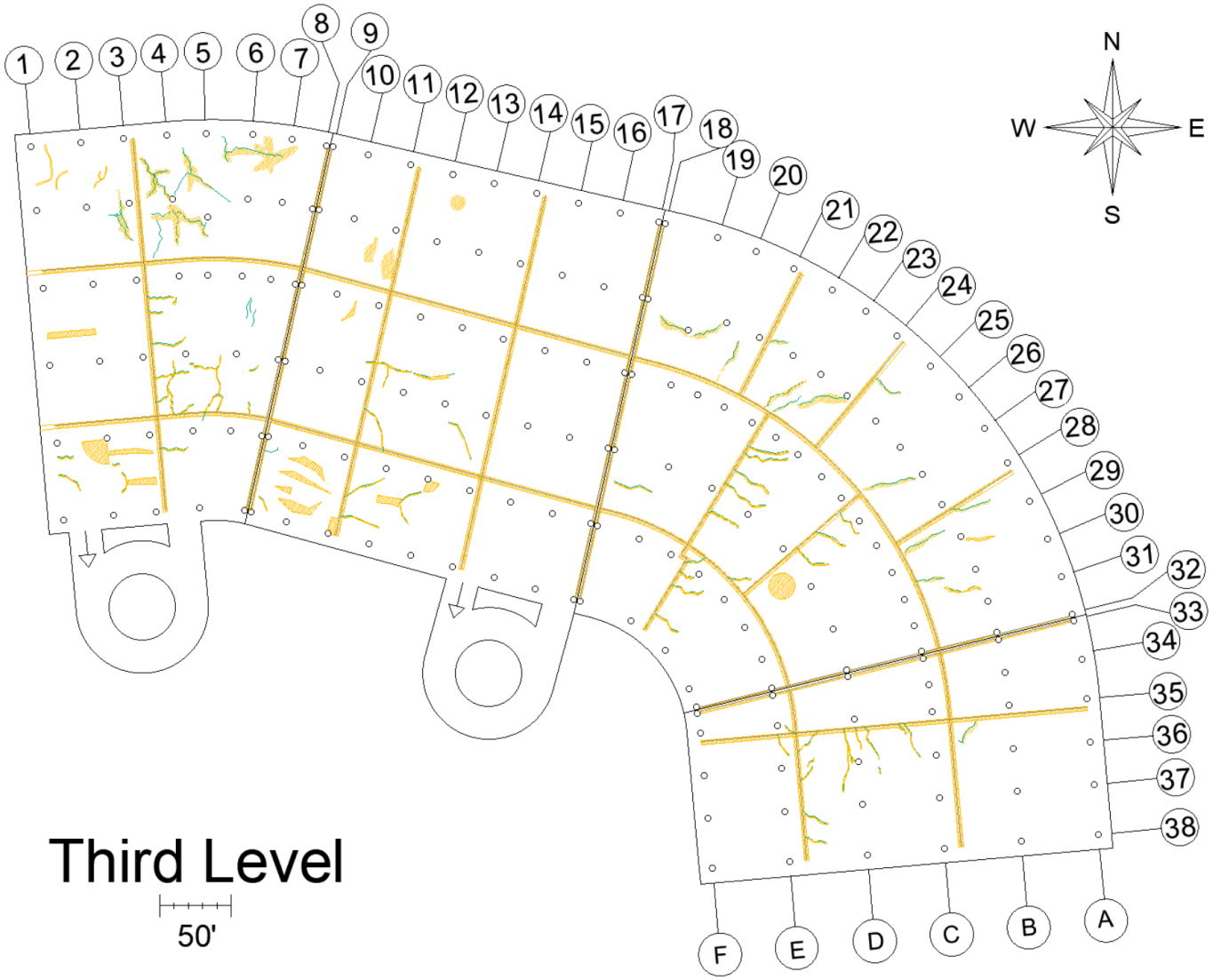

Figure 3-9 Crack map of the second suspended, reinforced silica fume concrete slab with green bottom-up cracks, yellow zones of efflorescence, and gray un-cracked epoxy-filled construction joints.

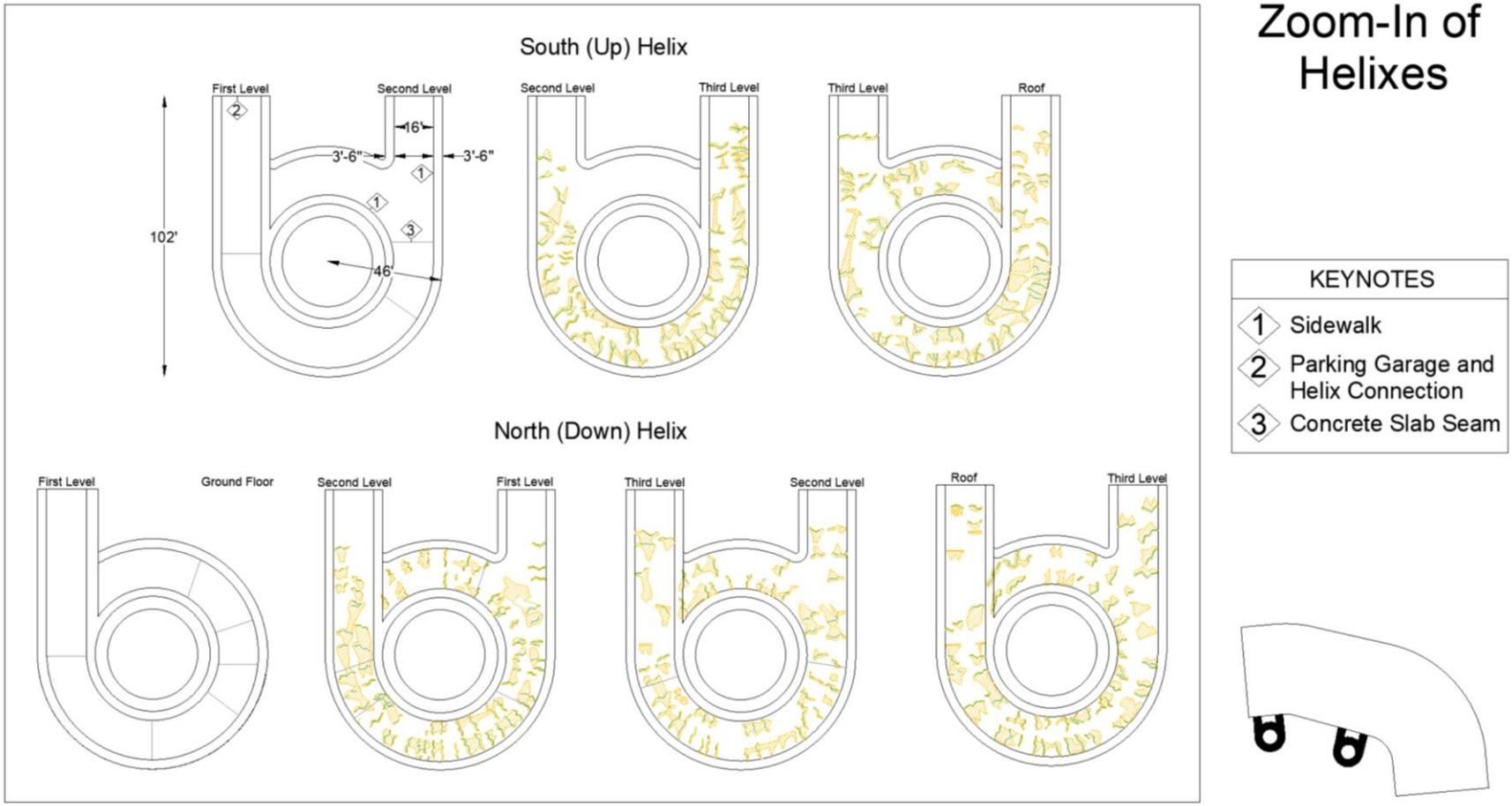

Figure 3-10 Crack map of the suspended, reinforced silica fume concrete helix ramps with green bottom-up cracks, yellow zones of efflorescence, and gray un-cracked epoxy-filled construction joints.

3.4 Crack Density

The total length of all of the cracks in the AutoCAD map drawings was measured by two separate individuals and used to obtain the average crack density. First, the individual calculated the size of the construction slabs using the AutoCAD program. Then, the individual measured and recorded a list in Excel of the length from AutoCAD of each separate crack. Finally, the statistics, like number of cracks, total sum of crack lengths, and crack density (crack length divided by the square foot of the construction slab), were calculated. These statistics reported in terms of each constructed slab and for each individual can be found in Appendix B. Table 3-1 shows a summary of the average crack density in the parking garage by structure type.

Table 3-1 Crack Density in Parking Garage

SLC Parking Garage Structure Type	Concrete Type	Reinforcement Type	Average Crack Density (ft/ft^2)	
Ground Floor	Plain	None	0.002	
Entrance Bridge	Micro-Silica	#7 epoxy-coated and PT cables	0.095	
Covered Suspended Slabs (1^{st}-3^{rd} floor)	Micro-Silica	#4 epoxy-coated and PT cables	1^{st} floor: 0.022 2^{nd} floor: 0.019 3^{rd} floor: 0.015	Overall: 0.018
Helixes	Micro-Silica	#4 epoxy-coated and PT cables	0.043	

The crack densities of the three suspended floors decreased with increasing level so that level one had the highest crack density and level three had the lowest of the three. From looking just at the micro-silica concrete with epoxy-coated and PT reinforcement in a covered slab or helix, there were high crack densities ranging from 0.015 ft/ft^2 to 0.043 ft/ft^2. These numbers are higher than what is reported in the literature study for a parking garage with three suspended slab stories of 0.009 ft/ft^2, however that study stated that was the criteria at which cracking would need to be sealed or repaired. Since it is likely that these more frequent cracks in this SLC parking garage

occurred so early in the structure and were already epoxy-filled, this comparison is no longer relevant. The entrance bridge which is uncovered and is the most closely related to what is seen in other bridge decks in the US with regard to environmental loading had a crack density of 0.095 ft/ft^2. This is lower than most other bridge decks reported in Appendix A, possibly because of the presence of the higher silica content, the use of post-tensioning or larger reinforcement bars, or just other climatic or loading factors.

The plain unreinforced concrete SOG that was covered had an extremely low crack density of 0.002 ft/ft^2. There is no way with just crack density information to single out the effect of the micro-silica slurry on the structural performance, particularly because the PT reinforcement is also noted in the literature as being a dominant crack density reducing methodology.

3.5 Locations of Chloride Profile Dust Samples and Cores

The following sites on the structure were identified, as mentioned in section 3.2, for which more detailed analysis (described in section 2.2) was performed. At these sites, Figure 2-2 for the ground level and Figure 3-11 to Figure 3-14 for the suspended levels and helix, show the specific locations for which chloride profile samples were taken and cores drilled. An example of the drilling can be seen in Figure 3-15. A summary list of the 15 cores taken and the 36 chloride depth sampling sites can be found in Appendix C.

At some of the sites, a specific grid pattern was laid out for which the Schmidt hammer and cover meter readings were also taken. Sites without the grid pattern were still measured for Schmidt hammer and cover depth readings, but not always at a specified grid pattern.

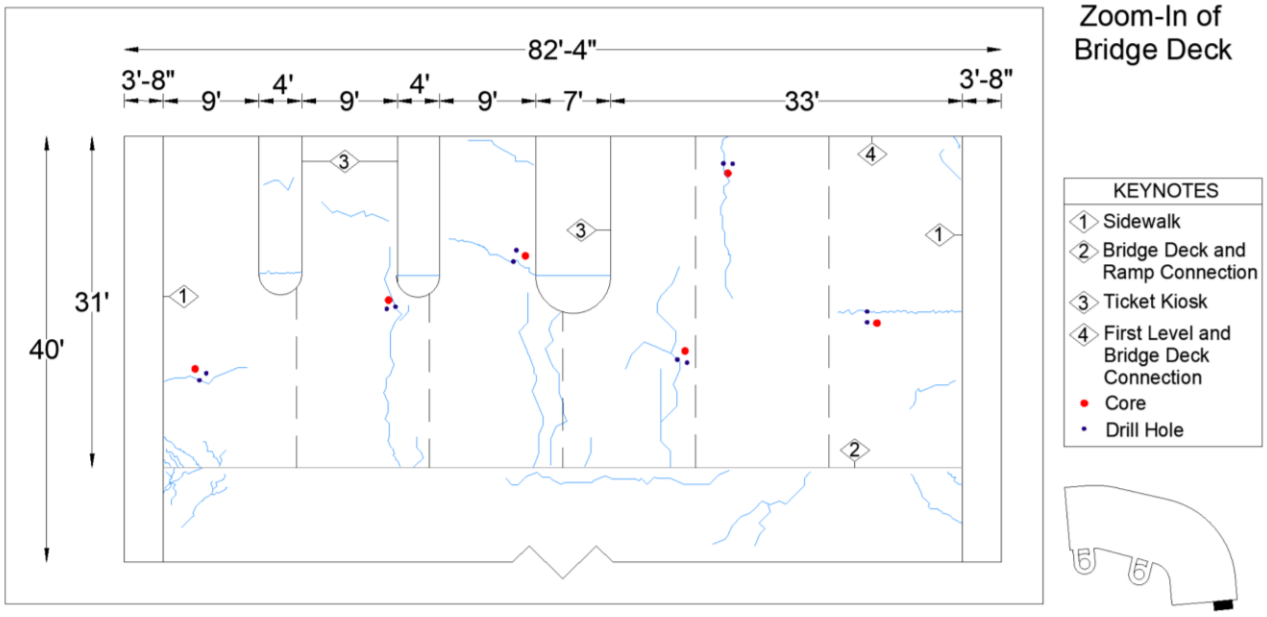

Figure 3-11 First floor entrance bridge detailed analysis site showing black dashed lines for the lane grid setup, red dots for core sample locations, blue dots for chloride-drilled sample locations, and top-down cracking (blue lines).

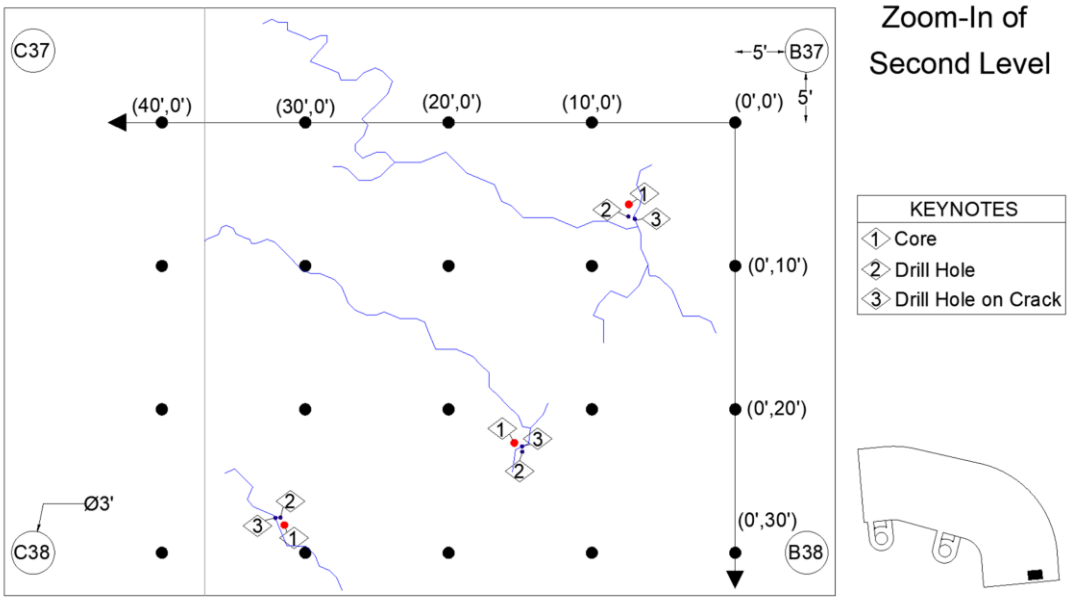

Figure 3-12 Second floor detailed analysis site showing the black dots for Schmidt hammer, cover depth, and VEI readings; red dots for core sample locations; and blue dots for chloride-drilled sample locations; and top-down cracking (blue lines).

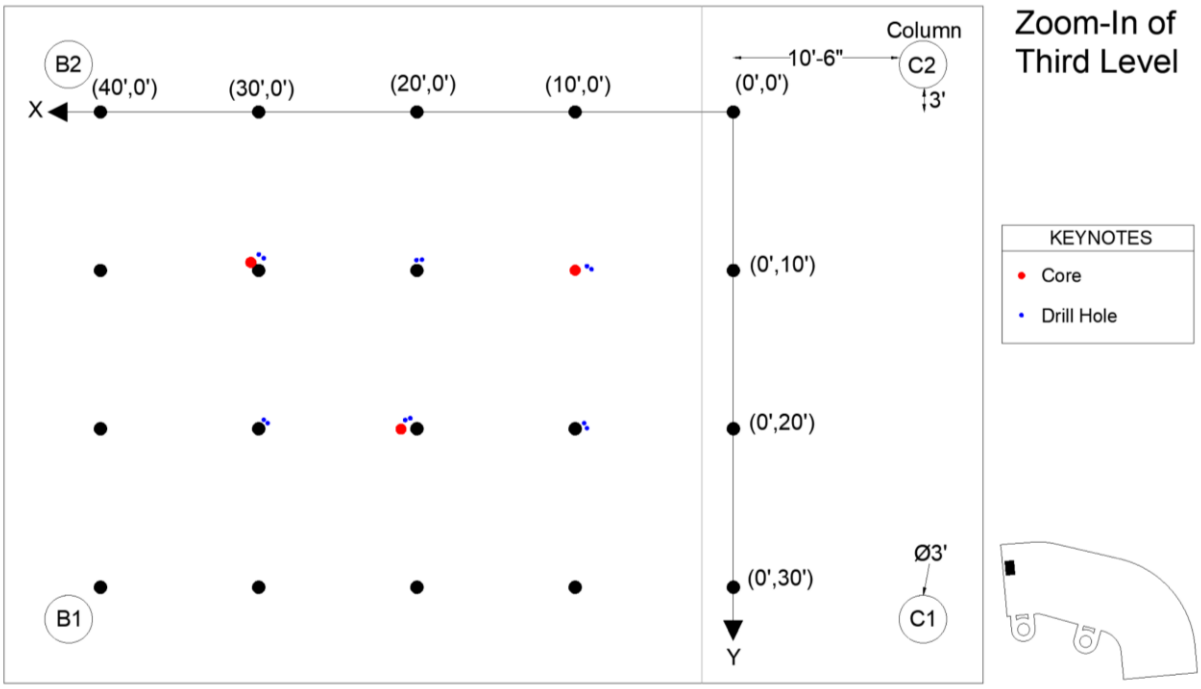

Figure 3-13 Third (top, covered) floor detailed analysis site showing black dots for Schmidt and cover depth readings, red dots for core sample locations, and blue dots for chloride-drilled sample locations. There were no cracks found in this site.

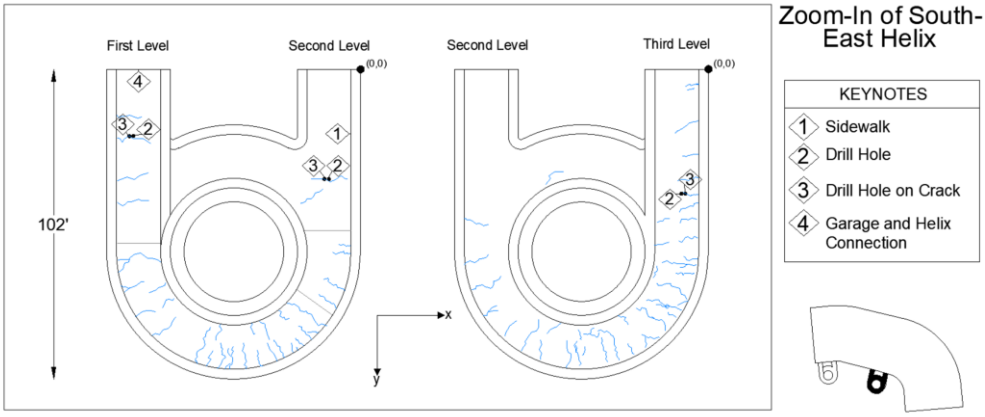

Figure 3-14 Helix (upward traffic, covered) floor detailed analysis site showing blue dots for chloride-drilled sample locations, and top-down cracking (blue lines). No cores were taken on the helix because of the inclined surface.

Figure 3-15 Photograph showing the drilling of the chloride penetration sample collection on the ground floor. Current image is of drilling the sample in the wheel-path (according to the paint) and at the epoxy-filled joint.

3.6 Schmidt Hammer and Cover Meter Depths

The Schmidt Hammer hardness test and cover meter depths were taken at each sampling location. Each Schmidt Hammer reading was taken on concrete that was first ground smooth. Ten readings were taken at each grid spot, and there were anywhere from 6 to 24 grid spots, meaning roughly 60 to 240 readings were taken at each location. The summary of the Schmidt Hammer readings can be seen in Table 3-2. It shows hammer impact readings of, on average, 57.

The rebound numbers for the tests performed on the SLC airport's parking garage all ranged between 50 and 60. Although they did not test concrete, Karaman and Kesimal (2015) studied rock samples with Schmidt rebound numbers between 50 and 60, and thus were used to estimate potential compressive strengths of over 23 ksi, shown also in Table 3-2. It is an interesting

note that even the plain (no micro-silica) concrete found in the ground floor has high rebound numbers similar to the micro-silica concrete.

Table 3-2 Summary of Schmidt Hammer Readings and Strength Predictions

Location	Type of Concrete	Number Readings	Average Schmidt Reading	Standard Deviation	Estimated Strength* (psi)
Ground Floor	Plain	120	55.00	2.79	21,410
Entrance Ramp	Micro-Silica	180	59.37	4.16	24,795
Second Floor	Micro-Silica	199	56.56	4.92	23,793
Third Floor	Micro-Silica	200	55.30	3.23	21,881
Helixes	Micro-Silica	30	56.67	4.52	22,840
Overall Micro-Silica Concrete			**57.0**	**4.5**	**23,327**

* Based on equation from (Karaman and Kesimal, 2015).

Cover depths were recorded on the same grid spots at each location in the garage. Two readings (one in the longitudinal and one in a transverse orientation) were taken at each grid spot. The reading locations did not necessarily correspond to reinforcement spacing, and thus at this time, it is uncertain whether the reinforcement picked up was an epoxy-coated rebar, a post-tensioned cable, or not even on top of a specific reinforcement but picking up a value from a neighboring reinforcement. The actual readings at each grid spot are listed in Appendix D. A summary of the cover depth measurements is shown in Table 3-3.

Table 3-3 Summary of Cover Depth Readings

Location	Type of Reinforcement	Number Reading Sites (two orthogonal readings per location)	Minimum Depth (in.)	Maximum Depth (in.)	Average Depth (in.)
Ground Floor	None	0	NA	NA	NA
Entrance Ramp	#7 Epoxy-Coated + PT Cables	18	2.20	5.00	3.16
Second Floor	#4 Epoxy-Coated + PT Cables	20	1.80	5.40	2.97
Third Floor	#4 Epoxy-Coated + PT Cables	12	1.90	5.80	3.45
Helixes	#4 Epoxy-Coated + PT Cables	3	3.25	4.65	4.05
Overall Cover Depth Readings (in.)			**1.8**	**5.8**	**3.2**

3.7 Summary

The results presented in this section show the locations of all visual cracks, exposed rebar, past cores, and efflorescence. Crack density calculations were performed and vary from 0.002 ft/ft^2 on plain unreinforced SOG segments to 0.095 ft/ft^2 on the micro-silica concrete with epoxy-coated rebar and post-tensioned strand entrance bridge deck. Other initial reported information is the Schmidt hammer readings which averaged around 57, or an estimated strength of over 23 ksi, and cover meter readings averaging between 1.8 and 5.8 inches from random locations on the structure surface.

4.0 PROJECT STATUS AND CONCLUSIONS

The old SLC airport parking garage was built between 1989 and 1991 and was completely demolished in 2020. The garage was built from concrete containing a 9% micro-silica slurry and was reinforced with rebar and post-tensioned tendons. The garage was one of the first larger structures in the United States built with a silica fume concrete.

Before demolition began, research teams from Brigham Young and Utah Valley Universities inspected, sampled, and took cores from the parking garage's concrete. As of Summer 2021, the concrete powder samples and GPR and VEI data are still being analyzed in BYU's engineering lab. This report discussed the history, background, visual inspections, crack densities, Schmidt Hammer results, and cover meter depth readings of the parking garage.

4.1 Completed Tasks to Date

Tasks that have been completed as of this report are:

- Crack location mapping and visual inspection of the parking garage
- Vertical electrical impedance scanning
- Pachometer (cover meter) scanning
- Schmidt Hammer readings
- Silica fume concrete powder sampling (on a crack and off a crack)
- Core samples at several locations and mixtures (plain and micro-silica) obtained

4.2 Findings

The SLC airport's old SFC parking garage had crack densities (0.014 ft/ft^2 and 0.095 ft/ft^2) that range between crack densities seen during first repairs of parking garages in California (0.009 ft/ft^2) and bridges in states with freeze-thaw cycles similar to Utah's (0.036 ft/ft^2 and 0.46 ft/ft^2). The garage's concrete is classified as being very high strength according to the original strength reports and confirmed with the recent measured Schmidt Hammer rebound numbers ranging between 50 and 60 across the entire garage.

4.3 Future Tasks

A publication regarding the VEI and GPR results will be created separately upon completion of the analysis from BYU. The following tasks are planned to be completed in the 2021-2022 academic year, through delegated effort between Brigham Young University, Utah Valley University, and the University of Toronto (U of T). Core samples that were taken from the structure will be strategically divided up to be analyzed for: rapid chloride permeability (ASTM C1202), bulk diffusivity (ASTM C1556), compressive strength estimation, carbonation depth, petrographic analysis for verifying air distribution near the surface, and x-ray diffraction analysis to verify any remaining calcium hydroxide content. The additional cylinders created at UVU with similar and alternative SCMs will be cut up like the core samples for multiple analyses. After all chloride and diffusion tests are completed, the values will be run through the Life-365 software and a report will be generated explaining how the real values predict the service life of the parking garage.

The following tests will be performed at each university.

At BYU:

- Chloride titration or concentration tests from powder samples
- Cores cut up and shipped out
- Rapid chloride permeability tests
- Carbonation depth (via split-tension and phenolphthalein)

At UVU:

- Recreate silica fume concrete mixture
- Creating alternative SCM (class F fly ash, pumice, and waste glass powder) mixtures to compare to silica fume
- Measuring fresh properties (slump, air) on the newly created cylinders
- Compressive strength tests
- Sending out for petrographic analysis (air content) and/or x-ray diffraction (calcium hydroxide remaining)

At U of T:

- Chloride titration or concentration tests from core samples
- Bulk diffusivity

REFERENCES

Aalami, B. Y. B. O., and Barth, F. G. (1989). "RESTRAINT CRACKS AND THEIR MITIGATION IN UNBONDED POST-TENSIONED BUILDING STRUCTURES." *ACI Special Publication SP-113*, American Concrete Institute, 56.

Bentz, E., and Hooton, R. D. (2008). *Testing of Concrete from Parking garages and Bridge Deck for the Silica Fume Association*.

Darwin, D., Khajehdehi, R., Alhmood, A., Feng, M., Lafikes, J., Ibrahim, E., and O'reilly, M. (2016). *Construction of Crack-Free Bridge Decks: Final Report*.

Earthquake Track. (2020). "Today's Earthquakes in Utah > 4.0M." <https://earthquaketrack.com/r/utah/recent?mag_filter=4>.

Epoxy Interest Group. (n.d.). "EIG: History of Epoxy-Coated Rebar - Epoxy Interest Group." <http://www.epoxyinterestgroup.org/about/history-of-epoxy-coated-rebar/> (Mar. 2, 2021).

Fidjestøl, P., and Dåstøl, M. (2008). "The History of Silica Fume in Concrete - from Novelty to Key Ingredient in High Performance Concrete." *IBRACON 50th Congresso Brasilerio de Concreto*, Insituto Brasilerior de Concreto, Salvador, Brazil, 78.

Ganapuram, S., Adams, M., and Patnaik, A. (2012). *Quantification of cracks in concrete bridge decks in Ohio District 3*.

Guthrie, W. S., Yaede, J. M., and Bitnoff, A. C. (2014). *Internal Curing of Concrete Bridge Decks in Utah: Mountain View Corridor Project*. *Utah Department of Transportation*.

Harley, A., Darwin, D., and Browning, J. (2011). *Use of Innovative Concrete Mixes for Improved*. *Kansas Department of Transportation, K-TRAN PROJECT JU-11-8*.

Hooton, D., Bentz, E., and Kojundic, T. (2010). "Long-Term Chloride Penetration Resistance of Silica Fume Concretes Based on Field Exposure." *Service Life Design for Infrastructure RILEM PRO 70*, 503–512.

Karaman, K., and Kesimal, A. (2015). "A comparative study of Schmidt hammer test methods for estimating the uniaxial compressive strength of rocks." *Bulletin of Engineering Geology and the Environment*, 74(2), 507–520.

Khosa, N. (2019). "History of Unbonded Post-Tensioned Concrete in Skyscrapers." *2019 Chicago 10th World Congress Proceedings - 50 Forward| 50 Back*, CTBUH, Chicago, 107–114.

Leistikow, R., Kramer, K. W., Lafikes, J., Khajehdehi, R., Feng, M., O'reilly, M., and Darwin, D. (2017). "Cracking and Durability in Sustainable Concretes Internal Curing and Supplementary Cementitious Materials in Bridge Decks." *Cracking and Durability in Sustainable Concretes*, American Concrete Institute, 1–20.

Ley, T. (2018). “What is epoxy coated rebar and why is it being banned? - YouTube.” *youtube*, <https://www.youtube.com/watch?v=xVDy84rR5Z8> (Mar. 2, 2021).

APPENDIX A: Comparison of Similar Bridges in the United States

Table A-1 Crack Densities, Reinforcement Type, and Pozzolan Used in Bridges in U.S.

State	Bridge (Baughn, 2019)	Date Placed	Age When Crack Analyzed (years)	Concrete Type	Reinforcement Type	Average Crack Density (ft/ft^2)
UT	Dannon Way, SB (Guthrie et al., 2014)	2012	2	20% Class F Fly Ash	No. 5, Epoxy-Coated Rebar Mat	0.20 (Darwin et al., 2016)
UT	8200 South, NB (Guthrie et al., 2014)	2012	2	20% Class F Fly Ash	No. 5, Epoxy-Coated Rebar Mat	0.36 (Darwin et al., 2016)
KS	WB Parallel Pkwy over I-635 (Leistikow et al., 2017)	2005	9	Subdeck: OPC Overlay: 7% Silica Fume	Reinforcing Bars	0.046 (Darwin et al., 2016)
KS	EB 103rd Street over US-69 (Leistikow et al., 2017)	2007	9	Subdeck: 20% Class F Fly Ash Overlay: 7% Silica Fume	Reinforcing Bars	0.12 (Darwin et al., 2016)
KS	K-52 over US-69 (Leistikow et al., 2017)	2007	8	OPC	Reinforcing Bars	0.21 (Darwin et al., 2016)
KS	SB US-59 over West Fork Tauy Creek (Harley et al., 2011)	2008	3	Subdeck: OPC Overlay: 7.8% Silica Fume	No. 5 Rebar	0.0649
OH	US-42 over SR 60 (Ganapuram et al., 2012)	2009	2	4.5% Silica Fume, 29% Slag	Reinforcing Bars	0.195
OH	SR 89 Over Branch Jerome Fork (Ganapuram et al., 2012)	2009	2	30% Slag	Reinforcing Bars	0.061

APPENDIX B: Specific Crack Lengths and Slab Areas

Table B-1 Ground Floor Crack Density Calculations for SLC Airport Parking Garage

Ground Floor							
Reading One (Maddie)				Reading Two (Thomas)			
Columns	Number cracks	Area (ft^2)	Crack Length (ft)	Columns	Number cracks	Area (ft^2)	Crack Length (ft)
Between Rows A&B							
1 to 3	0	7850.7	0	1 to 3	0	6427.61	0
4 to 9	3	12093	40.91	3 to 9	3	13010.37	40.92
10 to 11	0	6171.8	0	9 to 11	0	5502.01	0
12 to 14	0	9013.1	0	11 to 14	0	9209.97	0
15 to 17	0	8642.2	0	14 to 17	0	9408.5	0
18 to 21	1	9724.7	25.59	17 to 22	1	12194.29	25.95
22 to 24	1	7807.8	18.99	22 to 26	1	10685.19	18.99
25 to 28	3	10844.9	18.94	26 to 30	3	10790.07	25.66
29 to 32	3	10058.8	20.61	30 to 35	4	10605.79	77.91
33 to 35	2	6026.2	63.95	35 to 38	3	10247.28	33.47
36 to 38	1	9871.2	15.15				
Between Rows C&D							
1 to 3	0	8765.9	0	1 to 3	0	7024.73	0
4 to 8	0	10002.9	0	3 to 9	0	10749.45	0
9 to 11	0	6812.9	0	9 to 11	0	5970.73	0
12 to 14	1	9701.3	36.83	11 to 14	1	9689.97	30.86
15 to 17	1	8979.6	55.41	14 to 17	1	9486.2	61.38
18 to 22	0	9373	0	17 to 22	0	8449.05	0
23 to 26	0	7525.5	0	22 to 26	0	7064.39	0
27 to 32	0	10386.7	0	26 to 30	0	7139.79	0
33 to 35	0	4523.1	0	30 to 35	0	6973.41	0
36 to 38	4	10567.1	36.76	35 to 38	3	10268.04	101.03
Between Rows E&F							
1 to 3	0	6085.6	0	1 to 3	0	3502.51	0
4 to 8	0	4930.3	0	3 to 9	0	4030.09	0
9 to 11	0	4734.4	0	9 to 11	0	2981.3	0
12 to 14	0	6743.8	0	11 to 14	0	3248.67	0
15 to 17	0	6240.1	0	14 to 17	0	3113.16	0
18 to 22	0	4376.4	0	17 to 22	0	2810.91	0
23 to 32	0	7167.1	0	22 to 26	0	2218.52	0
33 to 35	0	2135.8	0	26 to 30	0	2217.6	0
36 to 38	2	7496.1	25.26	30 to 35	0	2144.55	0
				35 to 38	1	5127.93	12.59
Totals	**22**	**234,652**	**358.4**	**Totals**	**21**	**212,292**	**428.76**
Crack Density (ft/ft^2)			**0.0015**	**Crack Density (ft/ft^2)**			**0.0020**
Average Crack Density (ft/ft^2) for Ground Floor =							**0.0018**
Average Number of Cracks =							**22**

Table B-2 First Floor Crack Density Calculations for SLC Airport Parking

1st Floor							
Reading One (Maddie)				Reading Two (Thomas)			
Columns	Number cracks	Area (ft^2)	Crack Length (ft)	Columns	Number cracks	Area (ft^2)	Crack Length (ft)
Between Rows A&B							
1 to 3	7	7850.7	115.89	1 to 3	9	6427.61	148.3
4 to 9	30	12093	474.43	3 to 9	38	13008.7	659.03
10 to 11	3	6171.8	37.47	9 to 11	3	5559.51	37.53
12 to 14	4	9013.1	100.01	11 to 14	4	9208.93	99.36
15 to 17	14	8642.2	281.67	14 to 17	14	9274.03	309.7
18 to 21	7	9724.7	151.27	17 to 21	8	9333.63	165.32
22 to 24	5	7807.8	79.59	21 to 24	4	7952.93	92.03
25 to 28	4	10844.9	70.99	24 to 27	4	8188.02	72.74
29 to 32	5	10058.8	101.1	27 to 30	3	8256.96	59.18
33 to 35	4	6026.2	67.8	30 to 33	2	5580.54	41.92
36 to 38	5	9871.2	73.2	33 to 35	5	5021.9	77.85
				35 to 38	6	10250.09	90.89
Between Rows C&D							
1 to 3	3	8765.9	49.39	1 to 3	3	7024.73	72.75
4 to 8	5	10002.9	125.47	3 to 9	8	10762.27	197.08
9 to 11	12	6812.9	243.42	9 to 11	15	5971.2	372.52
12 to 14	24	9701.3	490.61	11 to 14	23	9723.6	572.67
15 to 17	20	8979.6	463.28	14 to 17	32	9475.32	671.43
18 to 22	14	9373	223.02	17 to 22	11	8447.35	234.86
23 to 26	5	7525.5	123.47	22 to 28	19	10572.97	387.32
27 to 32	18	10386.7	343.69	28 to 33	9	7385.6	187.08
33 to 35	1	4523.1	10.05	33 to 35	0	3226.95	0
36 to 38	11	10567.1	137.86	35 to 38	10	10269.62	120.39
Between Rows E&F							
1 to 3	12	6085.6	49.66	1 to 3	12	3562.54	44.85
4 to 8	3	4930.3	37.44	3 to 9	2	4030.09	27.53
9 to 11	1	4734.4	17.62	9 to 11	1	2981.3	17.62
12 to 14	11	6743.8	205.92	11 to 14	11	3245.67	206.07
15 to 17	10	6240.1	170.45	14 to 17	10	3113.16	179.35
18 to 22	3	4376.4	38.99	17 to 26	7	4995.59	97.29
23 to 32	4	7167.1	58.01	26 to 33	0	3400.9	0
33 to 35	2	2135.8	23.7	33 to 35	7	4346.89	114.58
36 to 38	6	7496.1	83.25	35 to 38	3	5127.93	21.06
Totals	**253**	**234,652**	**4448.72**	**Totals**	**283**	**215,727**	**5378.3**
Crack Density (ft/ft^2)			**0.0190**	**Crack Density (ft/ft^2)**			**0.0249**
Average Crack Density (ft/ft^2) for First Floor =							**0.0218**
Average Number of Cracks =							**268**

Table B-3 Second Floor Crack Density Calculations for SLC Airport Parking Garage

2nd Floor							
Reading One (Maddie)				Reading Two (Thomas)			
Columns	Number cracks	Area (ft^2)	Crack Length (ft)	Columns	Number cracks	Area (ft^2)	Crack Length (ft)
Between Rows A&B							
1 to 3	4	7850.7	74.4	1 to 3	4	6427.61	74.42
4 to 9	39	12093	538.71	3 to 9	49	13033.12	695.68
10 to 11	11	6171.8	195.58	9 to 11	11	5501.86	222.62
12 to 14	17	9013.1	257.75	11 to 14	20	9209.97	336.41
15 to 17	2	8642.2	45.05	14 to 17	2	9273.5	45.06
18 to 21	0	9724.7	0	17 to 21	0	9333.96	0
22 to 24	2	7807.8	18.86	21 to 24	1	7943.02	18.86
25 to 28	3	10844.9	81.71	24 to 27	2	8190.6	53.49
29 to 32	14	10058.8	226.03	27 to 30	9	8212.42	170.96
33 to 35	0	6026.2	0	30 to 33	6	5579.74	86.93
36 to 38	42	9871.2	775.31	33 to 35	0	5026.05	0
				35 to 38	42	10249.79	833.02
Between Rows C&D							
1 to 3	2	8765.9	40.5	1 to 3	2	7029.23	29.48
4 to 8	4	10002.9	35.12	3 to 9	3	10764.85	26.12
9 to 11	17	6812.9	233.79	9 to 11	22	6023.62	403.05
12 to 14	25	9701.3	485.51	11 to 14	32	9726.98	660.39
15 to 17	10	8979.6	130.38	14 to 17	11	9475.32	170.82
18 to 22	1	9373	8.98	17 to 20	1	4789.6	8.38
23 to 26	9	7525.5	141.19	20 t0 24	8	7045.5	129.6
27 to 32	3	10386.7	50.05	24 to 27	5	4779.06	61.82
33 to 35	0	4523.1	0	27 to 30	0	4729.86	0
36 to 38	1	10567.1	15.79	30 to 33	0	5070.2	0
				33 to 35	0	3226.95	0
				25 to 38	2	10287	34.61
Between Rows E&F							
1 to 3	4	6085.6	22.63	1 to 3	4	3501.9	22.63
4 to 8	0	4930.3	0	3 to 9	0	4030.09	0
9 to 11	8	4734.4	85.69	9 to 11	5	3046.97	70.95
12 to 14	14	6743.8	269.56	11 to 14	17	4871.07	383.78
15 to 17	0	6240.1	0	14 to 17	0	4722.93	0
18 to 22	0	4376.4	0	17 to 22	0	2810.91	0
23 to 32	1	7167.1	15.58	22 to 30	1	2180.96	15.58
33 to 35	1	2135.8	20.87	30 to 35	1	4346.89	20.88
36 to 38	3	7496.1	34.3	35 to 38	2	5127.93	15.48
Totals	**237**	**234,652**	**3803.34**	**Totals**	**262**	**215,569**	**4591.02**
Crack Density (ft/ft^2)			**0.0162**	**Crack Density (ft/ft^2)**			**0.0213**
Average Crack Density (ft/ft^2) for Second Floor =							**0.0186**
Average Number of Cracks =							**250**

Table B-4 Third Floor Crack Density Calculations for SLC Airport Parking Garage

3rd Floor							
Reading One (Maddie)				Reading Two (Thomas)			
Columns	Number cracks	Area (ft^2)	Crack Length (ft)	Columns	Number cracks	Area (ft^2)	Crack Length (ft)
Between Rows A&B							
1 to 3	4	7850.7	68.3	1 to 3	4	6427.61	68.45
4 to 9	53	12093	905.8	3 to 9	54	13033.12	933.15
10 to 11	12	6171.8	76.99	9 to 11	6	5501.86	40.33
12 to 14	0	9013.1	0	11 to 14	6	9208.93	36.6
15 to 17	0	8642.2	0	14 to 17	0	9274.03	0
18 to 21	10	9724.7	120.13	17 to 21	9	9333.63	120.13
22 to 24	7	7807.8	168.79	21 to 24	9	7943.02	175.95
25 to 28	4	10844.9	77	24 to 27	7	8190.6	109.27
29 to 32	11	10058.8	213.58	27 to 30	9	8212.42	177.88
33 to 35	0	6026.2	0	30 to 33	3	5579.74	73.23
36 to 38	2	9871.2	45.45	33 to 35	0	5026.05	0
				35 to 38	3	10250.09	60.51
Between Rows A&B							
1 to 3	0	8765.9	0	1 to 3	0	7029.23	0
4 to 8	20	10002.9	332.74	3 to 9	26	10764.85	427.6
9 to 11	1	6812.9	6.06	9 to 11	0	6023.62	0
12 to 14	5	9701.3	138.21	11 to 14	5	9726.98	142.47
15 to 17	0	8979.6	0	14 to 17	0	9556.78	0
18 to 22	3	9373	43.69	17 to 21	2	5903.26	36.64
23 to 26	6	7525.5	167.91	21 to 24	9	5974.89	239
27 to 32	4	10386.7	81.21	24 to 27	7	6032.96	161.98
33 to 35	0	4523.1	0	27 to 30	0	4729.86	0
36 to 38	16	10567.1	265.78	30 to 33	0	6273.9	0
				33 to 35	0	3226.95	0
				35 to 38	21	10271	374.59
Between Rows A&B							
1 to 3	6	6085.6	74.87	1 to 3	6	3502.5	72.79
4 to 8	3	4930.3	42.9	3 to 9	3	4028.53	42.92
9 to 11	2	4734.4	25.02	9 to 11	3	3046.97	36.2
12 to 14	3	6743.8	91.02	11 to 14	3	4871.07	91.02
15 to 17	0	6240.1	0	14 to 17	0	4722.93	0
18 to 22	0	4376.4	0	17 to 21	0	2810.91	0
23 to 32	4	7167.1	73.91	21 to 26	6	2180.96	110.66
33 to 35	1	2135.8	9.57	26 to 35	0	4346.89	0
36 to 38	1	7496.1	16.52	35 to 38	0	5127.93	0
Totals	**178**	**234,652**	**3045.45**	**Totals**	**201**	**218,134**	**3531.37**
Crack Density (ft/ft^2)			**0.0130**	**Crack Density (ft/ft^2)**			**0.0162**
Average Crack Density (ft/ft^2) for Third Floor =							**0.0145**
Average Number of Cracks =							**190**

Table B-5 Helix Crack Density Calculations for SLC Airport Parking Garage

Helixes			
Reading Two (Thomas)			
Floors	Number cracks	Area (ft^2)	Crack Length (ft)
South Helix (Up)			
First to Second	38	25111.8	742.79
Second to Third	109	25111.8	1664.67
Third to Roof	79	25111.8	1076.34
North Helix (Down)			
Ground to First	22	25111.8	621.74
First to Second	89	25111.8	1419.4
Second to Third	66	25111.8	1122.98
Third to Roof	67	25111.8	873.14
Totals	**470**	**175,783**	**7521.06**
Crack Density (ft/ft^2)			**0.04279**
Average Crack Density (ft/ft2) for Helixes =			**0.0428**
Average Number of Cracks =			**470**

Table B-6 Entrance Bridge Crack Density Calculations for SLC Airport Parking Garage

Entrance Bridge			
Reading Two (Thomas)			
Lane	Number cracks	Area (ft^2)	Crack Length (ft)
Entrance Bridge			
1	15	519.6	52.1
2	6	519.6	40.5
3	7	643.2	84.46
4	11	1320	106.68
Totals	**39**	**3,002**	**283.74**
Crack Density (ft/ft^2)			**0.09450**
Average Crack Density (ft/ft2) for Bridge =			**0.0945**
Average Number of Cracks =			**39**

APPENDIX C: Core and Chloride Profile Samples Obtained

Table C-1 List of Core Locations

Core Identification Number	Level	X Coord (ft)	Y Coord (ft)	Length of Core (in)	Description
G 10-5	Ground	10	5	7	
G 18-24	Ground	18	24	5.5	
G 40-5	Ground	40	5	6.75	
Lane 1	Bridge	8	17.5	5	
Lane 2	Bridge	22	3.5	6	
Lane 3	Bridge	24	20	6	
Lane 4	Bridge	41	9	5.5	
Lane 5	Bridge	54.25	15	6	
Lane 6	Bridge	72	19.5	2.75, 3	two separate pieces
L2 5-5	2	5	5	8.5	
L2 17-25	2	17	25	8.25	
L2 32-25	2	32	25	6.5	
L3 10-10	3	10	10	6.75	
L3 21-20	3	21	20	8.75	narrows at one end
L3 30.5-9.5	3	30.5	9.5	10	

Note: no cores taken from the Helix structure (not able to get coring rig to fit)

Table C-2 List of Drilled Chloride Profile Sample Locations

Locations of Chloride Profile Depths Taken			
Level	**X Coord (ft)**	**Y Coord (ft)**	**Notes**
Ground	10	5	high spot
Ground	18	25	wheel path (crack)
Ground	18	25	wheel path (no crack)
Ground	22	23	between wheel paths
Ground	38	21	parking stall
Ground	40	5	low spot
Bridge	8	17.5	crack
Bridge	8	17.5	no crack
Bridge	22	3.5	crack
Bridge	22	3.5	no crack
Bridge	24	20	crack
Bridge	24	20	no crack
Bridge	41	9	crack
Bridge	41	9	no crack
Bridge	54.25	15	crack
Bridge	54.25	15	no crack
Bridge	72	19.5	crack
Bridge	72	19.5	no crack
Helix G-1	84	22	
Helix G-1	84	22	
Helix 1-2	12	36	
Helix 1-2	12	36	
Helix 2-3	9	41	
Helix 2-3	5	41	
Level 2	5	7	crack
Level 2	5	7	no crack
Level 2	17.5	25	crack
Level 2	17.5	25	no crack
Level 2	32.5	26	crack
Level 2	32.5	26	no crack
Level 3	10	10	no crack
Level 3	10	20	no crack
Level 3	20	10	no crack
Level 3	20	20	no crack
Level 3	30	10	no crack
Level 3	30	20	no crack

APPENDIX D: Schmidt Hammer and Cover Meter Readings

Table D-1 Schmidt Hammer Readings for the Ground Floor

SCHMIDT HAMMER TEST FOR GROUND FLOOR OF PARKING GARAGE

Approx. X Coordinates (ft)	Approx. Y Coordinates (ft)	Schmidt Hammer Readings									
0	0	54	56	56	52	54	52	54	60	60	54
0	10	56	56	60	54	60	54	58	54	58	54
0	20	54	54	54	52	54	56	52	56	54	54
0	30	54	56	54	50	54	56	54	54	52	54
20	0	54	54	56	56	52	50	52	54	52	52
20	10	56	52	50	54	56	56	56	52	52	52
20	20	64	56	56	58	58	64	58	54	54	58
20	30	54	56	54	58	56	56	56	54	54	58
40	0	56	52	56	56	48	52	54	54	56	56
40	10	62	56	56	52	60	58	58	58	56	58
40	20	56	56	58	52	54	56	58	58	54	50
40	30	56	56	54	48	52	52	52	54	58	54

Data Entered by:	Trevor Pratt	**average**	**55.0**
Data Checked By	Jenessa Pace	**standar deviation**	**2.8**
		COV	**5%**

Table D-2 Schmidt Hammer Readings for the Entrance Ramp

SCHMIDT HAMMER TEST FOR ENTRANCE RAMP TO PARKING GARAGE

Lane	Point (inside lane)	Approx. X Coordinates (ft)	Approx. Y Coordinates (ft)	Schmidt Hammer Readings									
1	1	5.5	5.5	62	60	60	69	63	58	66	68	58	66
	2	5.5	15.5	64	62	59	61	60	60	60	60	60	62
	3	5.5	25.5	59	69	58	64	58	57	57	60	60	64
2	1	16.75	5.5	57	59	58	57	63	59	60	57	59	58
	2	16.75	15.5	68	64	59	68	61	60	62	66	63	60
	3	16.75	25.5	58	61	61	61	60	60	61	62	64	62
3	1	28	5.5	62	60	58	62	59	62	61	60	63	57
	2	28	15.5	61	63	61	61	64	62	62	65	60	62
	3	28	25.5	61	64	60	62	60	61	63	58	61	64
4	1	45.5	5.5	57	68	57	52	60	57	59	54	52	55
	2	45.5	15.5	52	50	52	52	53	50	52	53	62	54
	3	45.5	25.5	54	58	52	54	52	54	55	57	55	56
5	1	57.75	5.5	54	54	60	53	57	52	54	51	54	55
	2	57.75	15.5	57	55	59	57	60	57	54	54	55	58
	3	57.5	25.5	61	57	55	58	54	62	63	64	54	56
6	1	70	5.5	57	56	65	62	69	58	60	56	58	58
	2	70	15.5	62	57	60	60	68	65	68	64	58	61
	3	70	25.5	62	59	61	65	58	58	57	68	63	61

Data Entered by:	Trevor Pratt										**average**	**59.4**	
Data Checked By:	Jenessa Pace									**standar deviation**		**4.2**	
											COV	**7%**	

Table D-3 Schmidt Hammer Readings for the Second Floor

SCHMIDT HAMMER TEST FOR SECOND FLOOR OF PARKING GARAGE

Approx. X Coordinates (ft)	Approx. Y Coordinates (ft)	Schmidt Hammer Readings									
5	5	58	56	54	54	54	58	54	54	56	56
5	15	64	58	54	58	58	54	56	60	64	66
5	25	62	66	60	58	56	48	56	54	62	58
5	35	54	52	54	44	56	54	60	52	56	56
15	5	60	56	70	62	62	58	64	60	60	
15	15	52	54	62	48	60	58	54	56	56	56
15	25	52	58	62	54	56	56	48	58	54	58
15	35	52	52	54	52	56	44	50	46	52	50
25	5	62	64	58	58	56	58	58	60	60	56
25	15	60	48	58	58	60	52	48	58	62	60
25	25	54	64	62	58	58	54	60	54	60	58
25	35	48	50	42	58	52	52	54	46	54	64
35	5	56	56	64	52	52	54	58	60	58	58
35	15	58	60	60	60	62	56	58	58	68	62
35	25	58	56	56	58	58	60	68	68	60	56
35	35	48	48	58	52	56	56	54	44	58	56
45	5	56	58	58	52	58	54	54	58	66	68
45	15	58	68	54	54	58	48	58	62	58	56
45	25	52	54	58	60	68	50	54	58	58	56
45	35	50	48	60	60	54	56	50	56	54	54

Data Entered by:	Trevor Pratt								**average**	**56.6**	
Data Checked By	Jenessa Pace								**standar deviation**	**4.9**	
									COV	**9%**	

Table D-4 Schmidt Hammer Readings for the Third Floor

SCHMIDT HAMMER TEST FOR THIRD FLOOR OF PARKING GARAGE

Approx. X Coordinates (ft)	Approx. Y Coordinates (ft)	Schmidt Hammer Readings									
0	0	52	54	54	56	58	48	50	66	50	56
0	10	54	52	52	50	52	52	54	52	62	60
0	20	52	54	50	52	52	56	56	52	48	54
0	30	58	58	56	52	52	54	56	52	54	58
10	0	54	52	56	54	58	58	54	52	54	54
10	10	56	54	54	54	54	56	56	54	56	56
10	20	56	56	58	56	58	60	56	58	58	60
10	30	54	60	52	68	54	54	52	54	50	54
20	0	54	60	52	52	54	54	54	50	60	54
20	10	54	52	54	62	58	54	66	52	56	54
20	20	52	58	56	60	56	56	56	60	56	54
20	30	60	58	58	54	54	58	56	62	56	54
30	0	58	54	56	58	54	56	54	60	58	56
30	10	54	58	54	56	54	52	54	56	62	56
30	20	54	54	52	50	56	58	52	62	52	50
30	30	58	58	58	54	56	54	54	56	58	54
40	0	50	50	54	52	52	54	54	54	52	52
40	10	56	58	52	54	52	54	56	56	56	56
40	20	60	54	54	58	60	54	56	58	54	54
40	30	60	54	56	58	58	58	56	58	64	58

Data Entered by:	Trevor Pratt	**average**	**55.3**
Data Checked By	Jenessa Pace	**standar deviation**	**3.2**
		COV	**6%**

Table D-5 Schmidt Hammer Readings for the Helix Structure

SCHMIDT HAMMER TEST FOR HELIX PARKING GARAGE

Level of Parking Garage	Schmidt Hammer Readings									
1	55	56	52	54	52	56	55	61	64	56
2	60	56	58	54	64	60	60	57	57	67
3	53	49	59	59	53	57	44	57	57	58

Data Entered by:	Trevor Pratt	**average**	**56.7**
Data Checked By	Jenessa Pace	**standar deviation**	**4.5**
		COV	**8%**

Table D-6 Cover Meter Readings for the Entrance Ramp Structure

COVER METER READINGS FOR ENTRANCE RAMP TO PARKING GARAGE

				Cover Meter Reading (in)	
				Direction	
Lane	Point (inside lane)	Approx. X Coordinates (ft)	Approx. Y Coordinates (ft)	North-South	East-West
1	1	5.5	5.5	4.05	4.65
	2	5.5	15.5	3.70	4.60
	3	5.5	25.5	3.90	5.00
2	1	16.75	5.5	2.75	3.15
	2	16.75	15.5	2.40	2.60
	3	16.75	25.5	2.60	2.50
3	1	28	5.5	2.80	2.60
	2	28	15.5	2.70	2.55
	3	28	25.5	2.30	2.40
4	1	45.5	5.5	2.51	2.30
	2	45.5	15.5	2.20	2.55
	3	45.5	25.5	2.60	2.60
5	1	57.75	5.5	2.90	2.85
	2	57.75	15.5	2.75	2.60
	3	57.5	25.5	2.40	2.90
6	1	70	5.5	3.70	4.15
	2	70	15.5	4.20	4.75
	3	70	25.5	4.10	4.55
	Data Entered by:	Trevor Pratt	ave	3.03	3.29
	Data Checked By	Jenessa Pace	stdev	0.69	0.99
			cov	22.91%	30.09%
			min	2.20	
			max	5.00	
			average	3.16	

Table D-7 Cover Meter Readings for the Second Floor

COVER METER READINGS FOR SECOND FLOOR OF PARKING GARAGE			
		Cover Meter Reading (in)	
		Direction	
Approx. X Coordinates (ft)	Approx. Y Coordinates (ft)	North-South	East-West
5	5	2.60	2.25
5	15	2.35	2.25
5	25	2.40	1.80
5	35	2.90	2.75
15	5	2.50	2.20
15	15	5.25	5.20
15	25	4.50	2.35
15	35	2.60	2.80
25	5	2.90	2.75
25	15	5.40	5.10
25	25	4.50	2.95
25	35	2.90	2.45
35	5	3.35	2.60
35	15	3.00	3.85
35	25	2.05	2.50
35	35	1.80	2.10
45	5	2.80	2.75
45	15	2.90	3.05
45	25	3.10	2.95
45	35	2.20	2.10
Data Entered by:	Trevor Pratt		
Data Checked By	Jenessa Pace		
	ave	3.10	2.84
	min	1.80	
	max	5.40	
	average	2.97	

Table D-8 Cover Meter Readings for the Third Floor

COVER METER READINGS FOR THIRD FLOOR OF PARKING GARAGE			
		Cover Meter Reading (in)	
		Direction	
Approx. X Coordinates (ft)	Approx. Y Coordinates (ft)	North-South	East-West
0	0	2.80	3.25
0	10	4.25	4.70
0	20	3.85	5.05
0	30	3.05	2.25
20	0	2.95	3.05
20	10	5.80	4.45
20	20	5.80	4.75
20	30	3.30	2.75
40	0	2.10	2.00
40	10	3.15	3.05
40	20	3.10	3.45
40	30	2.10	1.90
Data Entered by:	Trevor Pratt		
Data Checked By	Jenessa Pace		
	ave	3.52	3.39
	min	1.90	
	max	5.80	
	average	3.45	

Table D-9 Cover Meter Readings for the Helix Structure

COVER METER READINGS FOR THIRD FLOOR OF PARKING GARAGE			
		Cover Meter Reading (in)	
		Direction	
	Level Of Parking Garage	Longitudinal	Transverse
	1	4.50	4.00
	2	4.65	4.00
	3	3.90	3.25
	ave	4.35	3.75
	min	3.25	
	max	4.65	
	average	4.05	
Data Entered By	Trevor Pratt		
Data Checked By	Jenessa Pace		